

A Major-II Project Report

on

Modeling and Simulation of Human Leg using Bond Graph

Submitted in partial fulfilment for the award of the degree

of

Master of Technology

in

Mechanical Engineering

with specialization in

Computational Design

by

DEEPAK KUMAR

(2K13/CDN/06)

Under the guidance

of

Dr. VIKAS RASTOGI

PROFESSOR



Department of Mechanical Engineering

Delhi Technological University, Delhi

July-2015



DELHI TECHNOLOGICAL UNIVERSITY

(Formerly Delhi College of Engineering)

Shahbad Daultpur, Bawana Road,

Delhi-110042

STUDENT'S DECLARATION

I **Deepak Kumar**, here by certify that the work which is being presented in this thesis entitled “**Modeling and Simulation of Human Leg using Bond Graph**” is submitted in the partial fulfilment of the requirements for degree of **Master of Technology (Computational Design)** Submitted in Department of Mechanical Engineering at **Delhi Technological University** is an authentic record of my own work carried under the supervision of **Dr. Vikas Rastogi**. The matter presented in this thesis has not been submitted in any other University/Institute for the award of Master of Technology Degree. Also it has not been directly copied from any source without giving its proper reference.

Signature of Student

This is to certify that the above statement made by the candidate is correct to the best of my knowledge.

Signature of Supervisor

The Master of Technology Viva-Voice examination of Mr. Deepak Kumar has been held on and accepted.

Signature of Supervisor

Signature of HOD

Signature of External Examiner



DELHI TECHNOLOGICAL UNIVERSITY

(Formerly Delhi College of Engineering)

Shahbad Daultpur, Bawana Road,

Delhi-110042

Certificate

This is to certify that the Major-II Project Report entitled “**Modeling and Simulation of Human Leg using Bond Graph**” is a bonafide work carried out by **Mr. Deepak Kumar (2K13/CDN/06)** of **M.Tech (Computational Design)** and submitted to Department of Mechanical Engineering, Delhi Technological University, Bawana Road, Delhi in partial fulfilment of the requirement for the award of the Degree of the Master of Technology under specialization in Computational Design under our supervision. It is further certified that the embodied work has not been submitted to any other institution for the award of other degree or certificate.

Dr. Vikas Rastogi

Professor

Mechanical Engineering Department

Delhi Technological University

Delhi - 110042

Acknowledgements

I would like to express my deep and sincere gratitude to my research supervisor, **Dr. Vikas Rastogi, Professor**, Department of Mechanical Engineering, Delhi Technological University, for giving me the opportunity to do research and providing invaluable guidance throughout this research. His dynamism, vision, sincerity and motivation have deeply inspired me. He has taught me the methodology to carry out the research and to present the research works as clearly as possible. It was a great privilege and honour to work and study under his guidance. I am extremely grateful for what he has offered me. I would also like to thank him for his friendship, empathy, and great sense of humour. Without the wise advice and able guidance, it would have been impossible to complete the thesis in this manner.

I would like to extend my thanks to Mr. Ashish Gupta, PhD Scholar, Delhi Technological University, without the help of whom the project is not able to make a possible indeed. I am also grateful to all faculty members of the Mechanical Engineering Department for molding me at correct time so that I can have a touch at final destination and to all my friends for moral support and encouragement; they had given to me during completion of dissertation work.

I am extremely grateful to my parents for their love, prayers, caring and sacrifices for educating and preparing me for my future.

Finally, my thanks go to all the people who have supported me to complete the research work directly or indirectly.

Deepak Kumar

M Tech. (COMPUTATIONAL DESIGN)

2K13/CDN/06

Abstract

The analysis of biomechanical leg is a very important clinical instrument to determine the nature of disease. Now a day many researchers analysed on biomechanics system such as human gait. The modelling and simulation of human gait is developed through various techniques such as vectorial mechanics Lagrange's equations, Kane method. These dynamic model of human body illustrate a different positional forces which is exerted on a human leg like a muscle, tendon, and other physiological effect. One of the techniques to simulate the human gait is bond graph modelling techniques. This technique avails to develop the model in multi energy domain. The generated differential equation is further used for simulation. .

The present work proposed a computational model of human gait through bond graph modeling and simulation work is carried out on Symbols Sonata[©] software. The fifth order Runge-Kutta method used for iteration. This work also revealed the introduction and different methodologies which used in the analysis of human leg e.g., inverse dynamic simulation and direct dynamic simulation and also explain the cyclic nature of gait.

Keywords: Human gait model, Bond graph modelling, Dynamic simulation.

CONTENTS

Student's deceleration	ii
Certificate	iii
Acknowledgements	iv
Abstract	v
Contents	vi
List of figures	viii
List if tables	xi
Chapter-1 Introduction	1
1.1 Motivation and background.....	1
1.2 Modeling.....	3
1.3 Bond Graph Modeling.....	4
1.3.1 Main advantages of bond graph techniques.....	5
1.4 Literature Review.....	5
1.5 Research gap.....	8
1.6 Objective of this research.....	8
1.7 Overview of this work.....	9
Chapter -2 Anthropometric measurement and kinematics	10
2.1 Model development.....	10
2.2 Inverse Solution.....	10
2.3 Development of Skelton system of human leg.....	11
2.4 Various forces acting on the link segment model.....	12
2.4.1 Gravitational force.....	12
2.4.1 Ground reaction force.....	12
2.4.2 Muscle and ligament force.....	12
2.4.3 Basic Link Segment Equation.....	12
2.5 Cyclic nature of gait.....	13
2.6 Phases in human gait.....	14

2.6.1 Events involve in walking	15
2.7 Body segment parameter	15
2.7.1 Selection of segment	16
2.7.2 Problems in identification of human leg	16
2.8 Anthropometric measurement.....	16
2.9 Mass and moment of inertia of segment.....	18
2.9.1 Mass of segment.....	18
2.9.2 Moment of inertia of segment	18
2.10 Determination of segment orientation	20
2.10.1 Definition of anatomical joint angle.....	21
2.12 Summary of the chapter	23
CHAPTER-3 Bond graph modeling of human leg	24
3.1 Introduction	24
3.2 Power variables.....	25
3.3 Basic element	25
3.4 Causality	26
3.5 Bond Graph Modeling of rigid beam.....	27
3.5.1 Procedure of modeling single rigid link in global coordinate system.....	28
3.5.2 Modeling of two rigid beams with articulated joint.....	29
3.5.3 Bond graph of 4 segment model of human leg.....	31
3.5.4 Integrated bond graph of right leg 4 segment model of human leg.....	32
3.5.5 Bond graph of 7 segment articulated lower limb of human.....	33
3.5.6 Integrated bond graph of 7 segment articulated lower limb of human	35
3.6 Summary of the chapter	36
CHAPTER-4 Dynamic analysis of model.....	37
4.1 Introduction.....	37
4.2 Simulation Environment	37
4.3 Symbols Sonata Software.....	37
4.4 Key Features of SYMBOLS Sonata Software are as follows	37
4.5 Simulation Properties	38

4.6 Runge-Kutta Gill method	39
4.7 Parameter Used In Simulation	39
4.8 Force generated in the lower segment	41
4.8 Force generated in the lower segment in horizontal direction	44
4.9 Summary of the chapter	47
Chapter-5 Result and discussion	48
5.1 Torque generated in segment	48
5.2 Generated moment about centre of mass	51
Chapter-6 Conclusions and future scope	54
6.1 Conclusions	54
6.2 Future scope.....	54
Appendix A.....	55
Appendix B	60
References	65

LIST OF FIGURES

Figure 1.1 The skeleton model of lower limb with ground reaction Force at the both foot.....	2
Figure 1.2: Process of modelling	4
Figure 2.1 Inverse dynamic simulation of human leg.....	11
Figure 2.2 Relations between anatomical model and link segment model.....	11
Figure 2.3 A link segment with applied forces and moment applied on it.....	12
Figure 2.4 Three plane in which study of human gait performed.....	14
Figure 2.5 Cyclic nature of human gait.....	15
Figure 2.6 Events involved in complete cycle of gait.....	16
Figure 2.7 Anthropometric measurement that is required in the body segment parameter.....	17
Figure 2.8 Thigh is shown in cylinder form with principle orthogonal axis.....	19
Figure 2.9 Orientation of segment in global coordinate system.....	20
Figure 2.10 Flat force plate measurement instrument.....	22
Figure 2.11 Force plate measurement data.....	23
Figure 3.1 A Lever example of transformer and bond graph notation.....	26
Figure 3.2 Angular velocity and velocity in global coordinate.....	27
Figure 3.3 Planer 2D rigid beam in global coordinate system.....	27
Figure 3.4 Bond graph modelling of rigid beam in global coordinate system.	28
Figure 3.5 Two 2D rigid beam in global coordinate system.....	29
Figure 3.6 Bond graph model of two 2D rigid articulated beam.....	30
Figure 3.7 Segment models of right leg 1, pelvis, 2 thigh, 3 shank, and 4 foot.....	31
Figure 3.8 Integrated model of 4 segment of human leg.....	32
Figure 3.9 skeleton system of human leg.....	33
Figure 3.10 Physical model of human lower limb 1pelvis, 2-5 thigh, 3-6 shank, 4-7 foot.....	34
Figure 3.11 Integrated 7 segment model.....	35
Figure 4.1 Force generated in the right hip along vertical direction (N).....	41
Figure 4.2 Force generated in the right leg along vertical direction (N).....	41
Figure 4.3 Force generated in left hip along vertical direction (N).....	42
Figure 4.4 Force generated in left leg along vertical direction (N).....	42

Figure 4.5 Force generated in right foot along vertical direction (N).....	43
Figure 4.6 Force generated in left foot along vertical direction (N).....	43
Figure 4.7 Force generated in right hip along horizontal direction (N).....	44
Figure 4.8 Force generated in left hip along horizontal direction (N).....	44
Figure 4.9 Force generated in right leg along horizontal direction (N).....	45
Figure 4.10 Force generated in left leg along horizontal direction (N).....	45
Figure 4.11 Force generated in right foot along horizontal direction (N).....	46
Figure 4.12 Force generated in left foot along horizontal direction (N).....	46
Figure 5.1 Torque generated in right hip due to vertical ground reaction force (N-m).....	48
Figure 5.2 Torque generated in left hip in flexion/extension direction (N-m).....	49
Figure 5.3 Torque generated in right shank in flexion extension direction (N-m).....	49
Figure 5.4 Torque generate in left shank in flexion extension (N-m).....	50
Figure 5.5 Torque generated in right foot in flexion extension (N-m).....	50
Figure 5.6 Torque generated in left foot in flexion extension (N-m).....	51
Figure 5.7 Moment in right hip (N-m).....	52
Figure 5.8 Moment in left calve (N-m).....	52
Figure 5.9 Moment in right foot. (N-m).....	53

LIST OF TABLE

Table 2.1 Anthropometry measurement of human lower limb.....	17
Table 2.2 Values of each segments anthropometric parameter.....	19
Table 2.3 Segment joint angle in global coordinate system.....	21
Table 3.1 Effort and flow system in bond graph.....	25
Table 3.2 Causality of different element.....	26
Table 4.1 Parameter used in simulation.....	39
Table 5.1 conversion of complete one cycle into time.....	48

1.1 Motivation and background

One of the major issues in the biomedical engineering field is to establish a mathematical model that is similar to the human leg, in a proper manner that gives us the opportunity to create a model, simulate or analyse of human movements like walking and running. Walking is achieved through a learning process that prepares muscles to full control the body for bipedal standing and walking. Generally scholars believe that human walking is not under full conscious control of the central nervous system; it can be assumed that the walking pattern has a very low level control in the spinal cord. During walking, one suddenly start to control walking when one have to avoid disturbance and when the normal walking path is not straight.

There have been performed many trial to induce walking in people with spinal cord injuries by using implanted electrodes in muscles. These electrodes are connected to a control system that provides a signal proportional to the motor force of the activated muscle necessary to create walking. Many biped walking robots have also been created and controlled using a combination of proportional-integral-derivative (PID) controllers and intelligent control.

It is difficult to perform human walking with mechanical models, so simulation and modelling becomes very useful design software that provide us the opportunity to collect more information of bipedal locomotion. This study is concerned with creating a model that can be easily modified and adapted to normal walking of human being. Now a days simulation and modelling is most popular instrument to study the complex dynamic system. There are many methods which is used to create a model of complex system. Bond graph modelling is one of the most appropriate method. Most complex models can be created and many factors, which affect the system can be analysed. Simulation result gives knowledge about a system actually work and can be modified system without creating a new real system.

In this work, a skeleton model of human leg proposed by Veera et.al [19], has been adopted and developed using bond graph technique. The study of biomechanics system is sometime more difficult in nature due to most complex system of human body. If the human

leg is analysed there are many factor, which is considered to create the model and validation of model is the most challenging work. Several assumptions must be taken to simplify the problem and to create the model.

The seven segment two dimensional model is developed in this work which may shown in the Figure 1.1

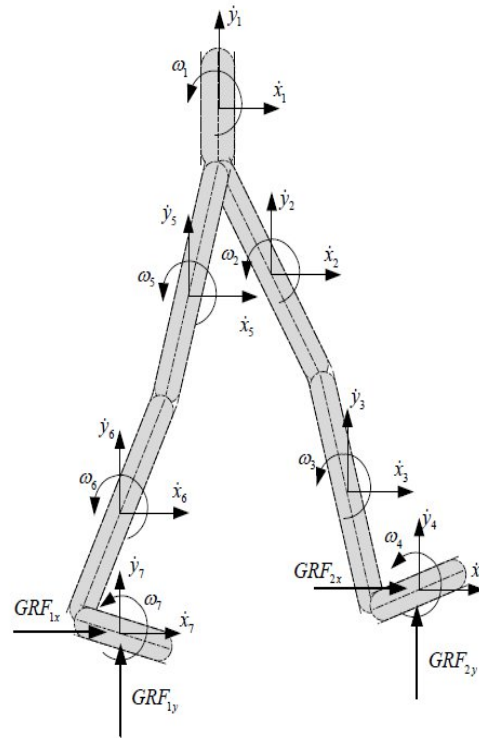


Figure 1.1: The skeleton model of lower limb with ground reaction force at both foot

The lower three segment represent foot, leg, and thigh the upper segment is pelvis which is connected to the thigh. The ground reaction force (GRF) is applied at both foot as external force to calculate the moment in each segment. This is simply a double support model of lower limb, that is why one may add ground reaction force at both foot. All the parameter, which is used in modelling and simulation is taken from the archival literatures.

Many parameters, which is used in simulation and modelling of leg is taken from experiment like mass, moment of inertia, length of each segment, joint angle and displacement etc. But some parameter like moment produced in each segment, power generation during walking cannot be directly measured. So, to find out these properties a model must be created which is similar to human leg and then find out the other parameter by

using inverse dynamic simulation. Model of lower limb gives a verity of information which may be used in the field of biomechanics. For example, if any joint of lower limb has to be replaced then computer model is used to give the various parameter, which is used in surgery and also such informations is very useful to the coach, surgeon, therapist and kinesiologist in their diagnostic assessments. The effect of training therapy or surgery is extremely evident at this level of assessment, although it is often obscured in the original kinematics.

For modelling and simulation, bond graph technique is used, which is very new in this area. Matthijsse et.al [1, 2], proposed the use of bond graph model in the modelling and simulation of human leg, two 13 segment model were presented by which single and double support can be simulated individually, but no direct simulation or inverse simulation result reported. Bond graph technique derived direct dynamic equation, which is same as derived by Euler or Newtonian approach. The fundamental used in formulation of bond graph of any system is exchange of energy by directional bond. This is achieved by dividing the system into small part and then connected by directional bond according to the flow of energy.

1.2 Modeling

Modeling is the process of producing a model, whereas a model is representation of the construction and working of some system of interest. One purpose of a model is to enable the analyst to predict the effect of changes to the system. On one hand, a model should be a close approximation to the real system and incorporate most of its salient features. On the other hand, it should not be so complex that it is impossible to understand and experiment with it. A good model is a judicious trade-off between realism and simplicity. An important issue in the modeling is the model validity. Model validation techniques include simulating the model under known input conditions and comparing model output with system output or some experimental data.

Most modern mechanical systems, however, form a part of multi-disciplinary system and are closely coupled with the hydraulic, magnetic, electrical or other kind of energy domains. Models of an integrated dynamic system using a hierarchical approach are advantageous. A systematic approach minimizes modeling mistakes by breaking the system model into small subsystems and components, which are manageable in size and complexity. The same components can be used repeatedly without having to build models of the same part again. For example, the axle component in the vehicle dynamics subsystem is built once and used for both the front and rear axle. In addition, with hierarchical modelling, models of

the same component with different complexity can be easily interchanged without changing the remaining structure of the model as shown in Figure 1.2

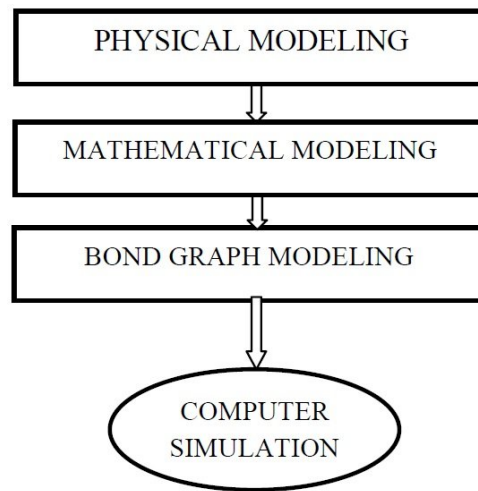


Figure 1.2: Process of modeling

1.3 Bond Graph Modeling

In the 1950s, H.M Paynter of MIT worked on interdisciplinary engineering project including hydroelectric plants, analog and digital computing, nonlinear dynamics, and control. He observed that similar forms of domain (for example electrical, fluid, and mechanical). Paynter incorporated the notion of an energy port into his methodology, and thus bond graphs were invented in 1959. Later on, bond graph theory has further developed by many researchers like Karnopp, thoma, Breedveld and Dauphi, Gawthrop and Smith, Mukharjee and Karmakar et.al [18], Brown and many more.

The bond graph method is a graphical approach to modelling in which component energy parts are connected by bonds that supply the transfer the energy between systems and components. The language aspires to express general class of physical systems through power interactions. The factor of power, i.e., effort and flow has different interpretation in different physical domain. Yet, power can always be used as a generalised coordinate to model coupled system residing in several energy domains. In bond graph, one needs to recognize only four groups of basic symbol i.e., three basic one port passive element inertance(I), capacitance (C) and resistance (R); two basic active element source of effort (SE) and source of flow (SF); two basic two port elements gyrator (GY), and transformer (TF); and two basic junction i.e., constant effort junction(0), and common flow junction(1).

The basic variables are effort (e), flow (f), time integral of effort (p) and time integral of flow (Q).

A physical system may be represented by symbol and lines, identifying the power flow paths. The lumped parameter elements of resistance, capacitance and inertance are interconnected in an energy conserving way by bonds and junctions resulting in a network structure. From the pictorial representation of the bond graph, the derivation of system equation is so systematic that it can be algorithmized. The whole procedure of modelling and simulation of the system may be performed by some of the existing software e.g., **ENPORT**, **Camp-G**, **SYMBOL-SONATA**, **20sim**, **COSMO** etc.

1.3.1 Main advantages of bond graph techniques

- Bond graphs can be used to describe simple linear and nonlinear.
- Bond graph provide a useful notation for the purpose of modeling physical systems.
- Systems with diverse domains are treated in a unified manner.
- Easiest way to communicate the description of energy flows in dynamic systems.
- By using power conservation properties of bond graph one may need to constraint velocities only and the forces will automatically be balanced.
- Graphical representation of complex models very clearly and unambiguously.
- Modal subsystems independently.

1.4 Literature Review

In this chapter the background of various investigation and the literature review are briefly presented. There are various studies which contributed by many researcher regarding the dynamic analysis of human lower limb.

Matthijssee et.al [1,2] has created bond graph model, which is a recent development as compare to the Newtonian and Lagrange method. In this concept one may portray the flow of power between sub elements of a physical system. The application of bond graphs to human locomotion modelling was first proposed by Matthijssee et.al [9, 10], in which two 13-segment models were described with which the single and double support phases could be individually simulated. Foot elevation was used to switch between models. However they does not give any inverse or direct dynamic simulation.

Winter et.al [4] proposed the most detailed solutions using inverse dynamics to obtain the joint torques, in which the body was modelled as an inverted pendulum in the A/P (anterior/posterior) direction. The analysis of standing pendulum model showed that the centre of pressure (COP) correlates the centre of mass (COM) to maintain balance control, and balance control was achieved by changing the COP of the feet. An effective net centre of pressure (COP_{net}) was introduced, which was defined as:

$$COP_{net} = COP_l \frac{GRF_l}{GRF_l + GRF_r} + COP_r \frac{GRF_r}{GRF_l + GRF_r} \quad 1.1$$

In the Eq. (1.1) subscripts l and r denote the left and right foot measurements respectively of the ground reaction force (GRF). The COP net values calculated from force plates readings were found to be very similar to those calculated for an inverted pendulum model. Various control strategies following different types of perturbations during standing were also analysed. For gait analysis, a 7-segment model using the Newton- Euler formulation with one segment for the upper part of the body was used. Using the inverted pendulum model, the effect of the combined head, arms and trunk (HAT) segment was investigated, and was found to have significant implications for the dynamic balance of the whole system. The results reported in this paper are most significant as one model is sufficiently used for both single and double support phases. Three dimensional kinetic analysis results are reported by Winter et.al [4] which shows the importance of the frontal and transversal plane moments and power in maintaining balance.

Pezzack et.al [9] used Newtonian mechanics to develop a model and analysis of this model is done by using direct dynamic simulation and he further validated his model using three steps:

- i. Computational accuracy against hand calculations.
- ii. Ground reaction forces (GRFs) estimated by the model against force plate measurements.
- iii. The accuracy with which the model predicted zero GRF at the distal end of the swing limb during the single support phase was verified.

The results reported were found accurate within 15%.

Kingma et.al [8] validated their 3-D model in two steps: firstly by comparing the ground reaction force (GRFs) predicted by the model with those values which was predicted by force plate measurement data, and then by comparing the torques at the hip joint resulting

from bottom-up and top-down mechanical analysis. It has been concluded that the most effective method of validating the model is by comparison the ground reaction force data predicted by model with force plate measurements.

Risher et.al [10] has presented a simple inverse dynamics solutions in direct dynamics simulations. It has been suggested that neither measurements nor derivative estimation errors can lead to simulation failure. Different models for the inverse and direct dynamics simulation has been used and it has been concluded that insufficient control signal are the reasons for simulations failure. By mapping estimated inverse dynamic torques into continuous signals and using them as input signal for direct dynamic simulation will result in a successful simulation. They used for mapping additional unspecified parameters in order to interpolate between samples. Joint torques and COPs resulting from the inverse dynamics algorithm are usually used in gait analysis, which are the first step to direct dynamics simulations.

Amirouche et.al [17] showed that modelling the constrained equations is the key element for reproducing human locomotion. Using dynamic equations for a 17-segment model, the GRFs were calculated without using force plates. The main emphasis in their paper is on the estimated torques obtained through the inverse dynamics, which recognizing the limitations due to prescribed motion (experimental data) on the joint torques. The simulations limited to the swing phase using a 6-segments model. It has been claimed that the method is applicable to experimental data that can describe any physical activity of the human body.

Tashman et.al [14] has presented a 4-segments 3-D model with 8 DOF for the analysis of gait. A reciprocating gait orthosis (RGO) is used to assist the subject when walking, which makes the kinetic analysis results difficult to be used for comparison. An optimization technique to find control forces and torque was used to minimize the error between the simulation and experimental results. The weights of the cost function are determined by trial and error procedure. Minimizing the error between the simulation and the experimental results, optimal control forces and torques revealed a low energy strategy to obtain a simulation very close to the experimental data. The significance of this work is in the potential of verifying the accuracy of the model by checking the difference between optimal values and the kinetics calculated.

Runge et.al [13] has studied an inverse dynamic and showed that using optimal linear system theory, specifically the LQF (linear quadratic follower) to estimate net joint torques

(NJT) the experimental measurements are closely reproduced as experimental data. Their method requires a very good initial guess of the NJT to converge to a stable system. Similarly, Runge and Kuo et.al [16] has used a least square estimation approach to improve torque's precision. The results show that for the upper part of the body (hip, arm and trunk) the estimated torques improved compared to torques estimated using simple inverse dynamics.

An example using intelligent control to predict control torques or muscles force used in direct dynamic simulations, were presented by Taga et.al [15] he generated the control torques using rhythm-generating neural networks. A very complex control system to provide dynamic stability of an 8-segment model, based on integrating realistic and neural dynamics and a sensory motor mechanism has been used. Armand [20] in his work shows that the hip elevation strategy is the key control element in stepping over obstacles. Using a multi-objective optimization approach to generate the limb trajectories at stepping over obstacles, several initial conditions and muscles pulse parameters are generated. Four objective functions were created to investigate the possible objectives that CNS (central nervous system) will consider when stepping over an obstacle by using a neuro-fuzzy-genetic optimization, any novice ambulatory is trained to learn to associate visual inputs, obstacle size and location to step over an obstacle. The genetic algorithms are used to optimize the membership parameters for the square neurons from the last layer of the neural-fuzzy system.

1.5 Research gap

All the studies presented in literature review has mainly the classical method to develop mathematical model of human gait e.g., Newtonian and Lagrange method. Most of them used direct dynamic simulation to develop model and they validate their model with force plate measurement only Winter et.al [4], used inverse dynamic simulation to elaborate human torque. In most of the studies the tendon and ligament force in the modelling has not been considered and 3D model of human gait is not developed accurately. Some researchers have developed 3D model of human gait, but with different methodology. None of this researchers used bond graph technique to simulate human gait model. The model proposed by Matthijssee et.al [1, 2], give some glimpsis of the bond graph technique applied to the gait model, but he had not simulated the model to diagnose the behaviour of gait.

1.6 Objective of this research

1. To develop a dynamic model of human gait system through bond graph technique.

2. To simulate the model with different conditions and analyse various environmental effect on the system.

1.7 Overview of this work

Chapter 2 contains various methodology used in the formulation of model and description of human leg. Chapter 3 contains bond graph modelling of human gait system. Chapter 4 contains dynamic analysis of model by using SYMBOL-SONATA software. Chapter 5 contains Results and discussion. Chapter 6 contains conclusion and future scope

ANTHROPOMETRIC MEASUREMENT AND KINEMATICS

2.1 Model development

The validity of any model is depend upon anthropometric data such as mass, moment of inertia, Centre of Mass (COM) of each segment. These data depend generally on person's height weight and sex. According to these anthropometric data following assumptions have been made for the development of a valid model:

- Each lower segment has a fixed mass, which is located as a point mass at the centre of mass.
- The location of centre of mass of each segment is fixed throughout the motion.
- The joint are considered to be a articulated joint
- The mass moment inertia is constant during the motion about the mass centre (or distal, proximal joint).
- The distance between each joint is constant during the motion or one may consider that length of each segment is fixed.

2.2 Inverse Solution

Now a day transducer can calculate reaction force and moment, when they are planted surgically to the body. However, this technique is applied only in animal experiments and only to a limited event. In case of human being, it is not possible to measure these data by using transducer. So for human being if one may have correct anthropometric data and kinematics data, one may develop a reliable link segment model. With this model and accurate kinematic data, we can predict the net forces and muscle moments that caused the movement one may just observed. Such an analysis technique is called an **inverse solution**. It is extremely valuable, as it allows one to estimate variables such as joint reaction forces and moments of force. Such variables are not measurable directly.

A schematic diagram of inverse solution in which kinematics, kinetics and anthropometric data is given to a link segment model, moment, joint reaction force and kinetic and potential energy of lower limb can be easily find out as shown in Figure 2.1.

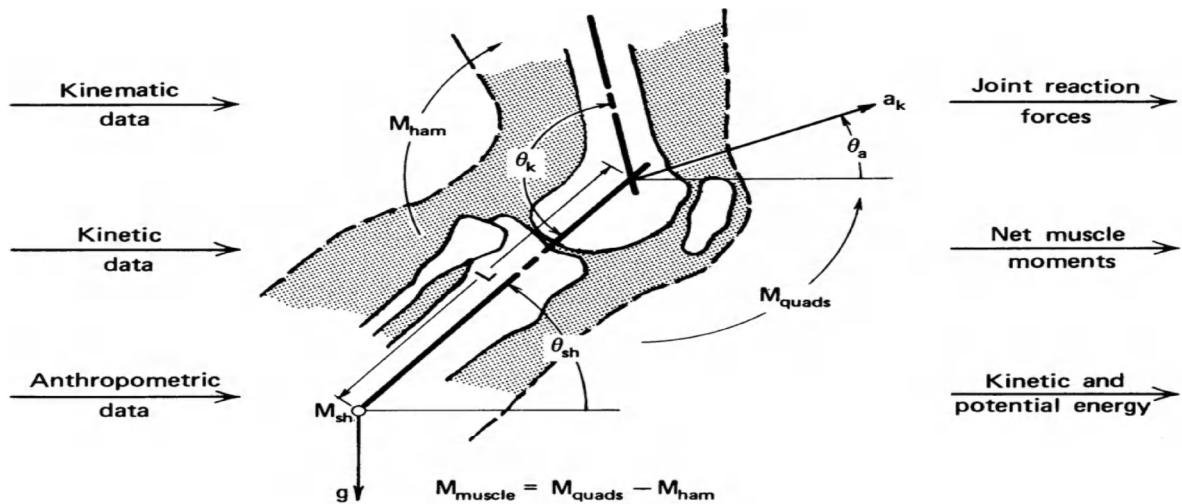


Figure 2.1: Inverse dynamic simulation of human leg [4]

2.3 Development of Skelton system of human leg

In the human body lower limb is the combination of pelvis, thigh calf and foot, which are joint to each other in a manner so that they can individually move relative to each other. Pelvis is rigidly attach to the rest of other upper part (HAT, head arm and trunk) and then thigh attach to pelvis at hip joint. Again shank attach to the thigh at knee joint and foot attach to the calf at the ankle joint. Here, figure 2.2 shows relationship between anatomical model and link segment model. Joint are replaced by articulated joint and segment are considered to be rigid beam in which their mass and moment of inertia located at their centre of mass.

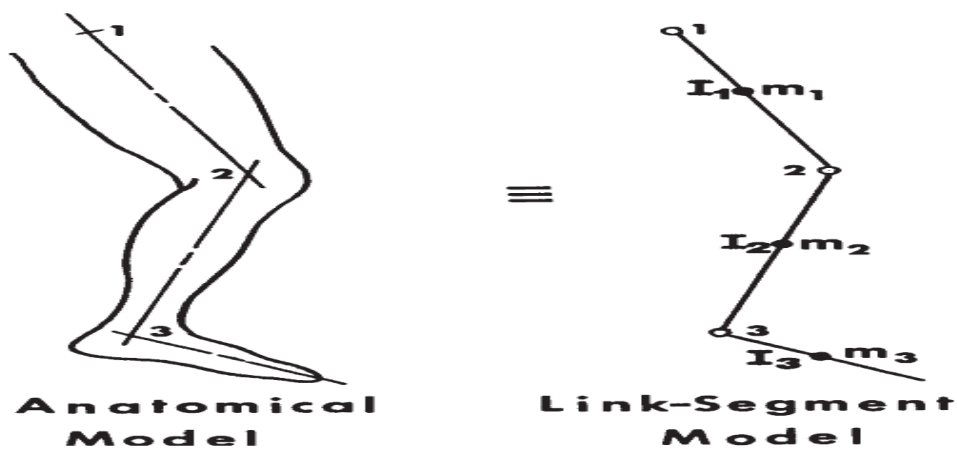


Figure 2.2: Relations between anatomical model and link segment model [4]

2.4 Various forces acting on the link segment model

2.4.1 Gravitational force

Gravitational force generally acts downward at the centre of mass of each segment and simply equal to the value of product of mass and gravitational acceleration.

$$F = \text{mass of segment} * \text{gravitational acceleration (g)}$$

2.4.1 Ground reaction force

The ground reaction force or any external forces are measured by force transducer. So for normal walking, one heels strike to the ground for balance of the human body, a reaction force is generated on the foot that is called ground reaction force. The ground reaction force is distributed all over the surface of foot, and they must act at the centre of mass of the foot.

2.4.2 Muscle and ligament force

The net effect of muscle and ligament force at a joint can be calculated in the term of net muscle moment acting at that joint. But in this work, no muscle and ligament force is considered. Muscle and ligament force calculation is very difficult task, one moves very slowly it is very accurate. However if one moves very fast, the roll of tendon take place and accuracy is less.

2.4.3 Basic Link Segment Equation

Every segment acts individually under the external and internal forces which acts the distal ends and the force due to gravity. This force is equal to product of mass and gravitational acceleration as shown in Figure 2.3

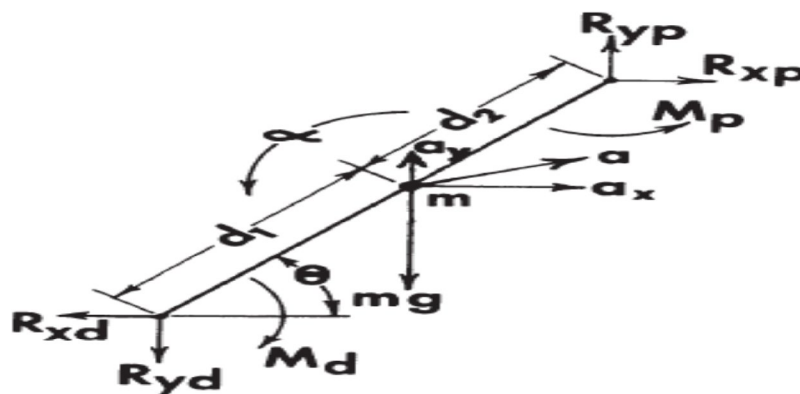


Figure 2.3: A link segment with applied forces and moment applied on it [4]

In the Figure 2.3, the following nomenclature is known and used:

a = Acceleration of segment at centre of mass

θ = Angle made by segment in the plane of movement

α = Angular acceleration of segment COM

R_x, R_y = Reaction force at the distal end due to the external forces

M_d = Net moment acting at distal end

The other unknown parameters are as follows:

R_p = Reaction forces acting at the proximal joint

M_p = net moment acting at the proximal joint

The following equation are being used

$$\text{Force} = M * a \quad 2.1$$

$$\text{The net moment of segment about COM} = I * \alpha \quad 2.2$$

$$\Sigma \text{Moment} = \text{Rate change of angular momentum} \quad 2.3$$

2.5 Cyclic nature of gait

Dynamics of gait takes a top down approach to describe the human gait model. The process starts from the central nervous system and end with, when heel strike with the ground and generation of ground reaction force take place. The joint force and joint moment causes the rigid skeleton segment (thigh, calf, foot) to move and exert external forces to the environment.

The following steps must be performed in case of normal waking.

- I. Command generated from central nervous system and transmitted to the peripheral nervous system.
- II. Contraction of muscle to developed the tension.
- III. Generation of force and moment at the synovial joint.
- IV. Movement of segment.
- V. And finally generation of ground reaction forces to balance the body.

There are mainly three plain of human body, which have been defined as (i) frontal plane, (ii) sagittal plane and (iii) transverse plane. But many researchers focus only on the sagittal plane because many movements take place in this plane only as shown in Figure 2.4.

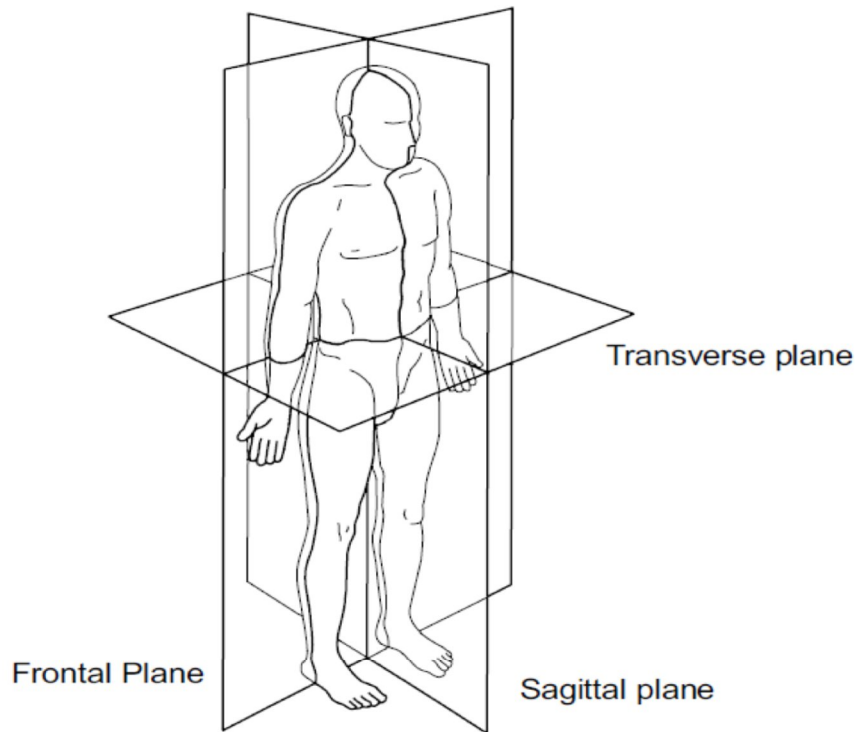


Figure 2.4: Three plane in which study of human gait performed [11].

In walking, following two action are performed in cyclic nature.

1. The periodic movement of foot from one position to the next position.
2. Generation of ground reaction force to balance the body.

The above two basic element is required in any form of bipedal walking; the periodicity of gait is pure natural tendency.

2.6 Phases in human gait

There are generally two main phase in the gait cycle (i) stance phase in which foot is on the ground and (ii) swing phase when foot is no longer in contact with the ground. As one may see in the Figure 2.5 that stance phase may be subdivided into three subparts.

- i. First double support- when both feet are on the ground.
- ii. Single limb support phase- when left foot is in swing phase.
- iii. Second double support- when both feet again touch the ground.

Figure 2.5 shows a cyclic nature of human gait from initial contact to the terminal swing of right leg and this process is continuously repeated over and over. It start from initial contact then loading response, mid stance, terminal stance, pre swing and finally swing phase (initial, mid, terminal swing) start.

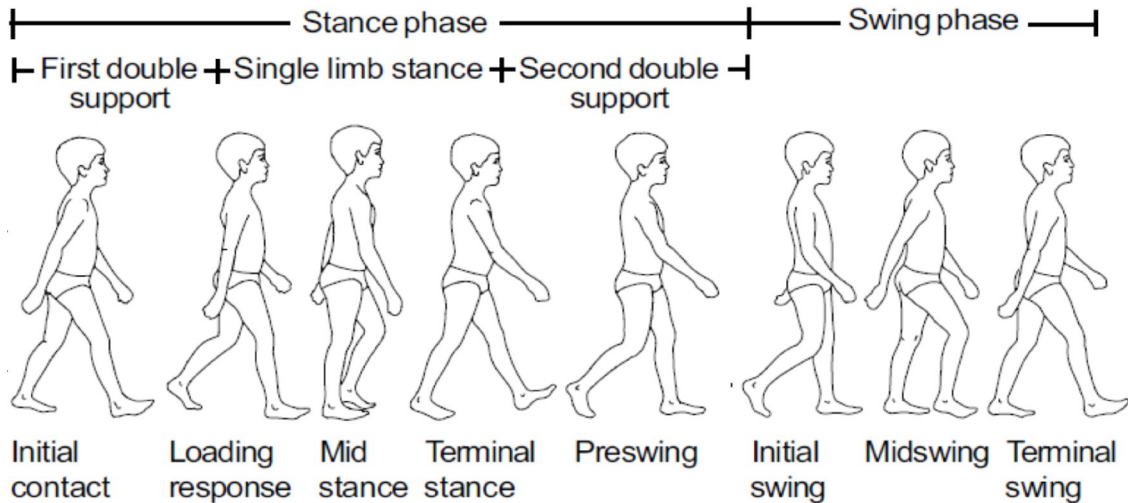


Figure 2.5: cyclic nature of human gait [11]

2.6.1 Events involve in walking

Gait cycle has been divided into eight main events, in which five are during stance phase and three are during swing phase as shown in Figure 2.6

- i. Heel strike initiates the gait cycle and shows the point at which the body's CG at lowest height.
- ii. Foot flat is the position when total surface area of foot is touches the ground.
- iii. Mid stance occur when the left foot (in swing position) passes the right foot (in stance position) and this time CG is at highest position.
- iv. Heel off occur when heel leaves the ground.
- v. Toe off is the final position of stance phase and finally foot leaves the ground.
- vi. Acceleration of foot begins as soon as foot leaves the ground.
- vii. Mid swing occurs just after the acceleration of foot and in this position right foot is coincident with the other foot mid stance position.
- viii. Finally for next heel strike foot decelerate.

2.7 Body segment parameter

The main problem in the analysis of gait is determine the body segment parameter i.e. mass of each segment in kilogram of each segment (pelvis thigh calf foot), location of centre of gravity of each segment relative to proximal and distal joint and moment of inertia of each segment about the interested axis.

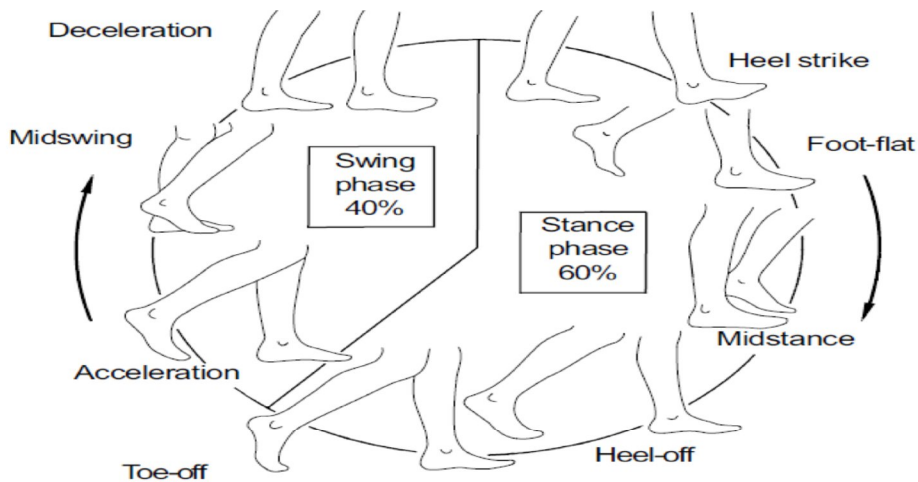


Figure 2.6: Events involved in complete cycle of gait [11]

2.7.1 Selection of segment

Another problem in gait analysis is selection of segment; here we have chosen seven segments (e.g., pelvis, thigh calf and foot). Here we have made some assumption that these are rigid segment and generally do not change in dimension during the movement but one may know that foot is not a single rigid segment so this may be the limitation of the model.

2.7.2 Problems in identification of human leg

There are several methods, which are used in the estimation of body segment parameter.

- i. Cadaver averages in this total body weight is used in the prediction of other segment which is not specific for individual person, this is the main limitation of this method.
- ii. Generally the reaction board technique is very long process and it is not suitable for measurement of segment masses and centre of gravity independently.
- iii. Mathematical modeling has main limitation of computational time. It takes more time to give results/output.
- iv. Scan using gamma rays is a very accurate method and have some limitation i.e. radiation exposure and very costly.

2.8 Anthropometric measurement

There are many anthropometric parameters, which are required in defining body segment parameter (mass, moment of inertia). Figure 2.7 shows the basic parameters, which are required in the measurement of segment parameter.

Table 2.1 contains the measurement of human lower limb [11] that is required in the anthropometric calculation as shows in the equation of the mass and moment of inertia. All the values are directly measured from body in gait lab.

Table 2.1: Anthropometric measurement of human lower limb

Number	Anthropometric measurement	Value	Units
1	Total body mass	64.90	Kilogram
2	ASIS breadth	.240	Metre
3	R. Thigh length	.460	Metre
4	L. Thigh length	.465	Metre
5	R. Calf length	.430	Metre
6	L. Calf length	.430	Metre
7	R. Foot length	.260	Metre
8	L. Foot length	.260	Metre
9	R. Malleolus height	.060	Metre
10	L. Malleolus height	.060	Metre
11	R. Malleolus width	.074	Metre
12	L. Malleolus width	.073	Metre
13	R. Foot breadth	.098	Metre

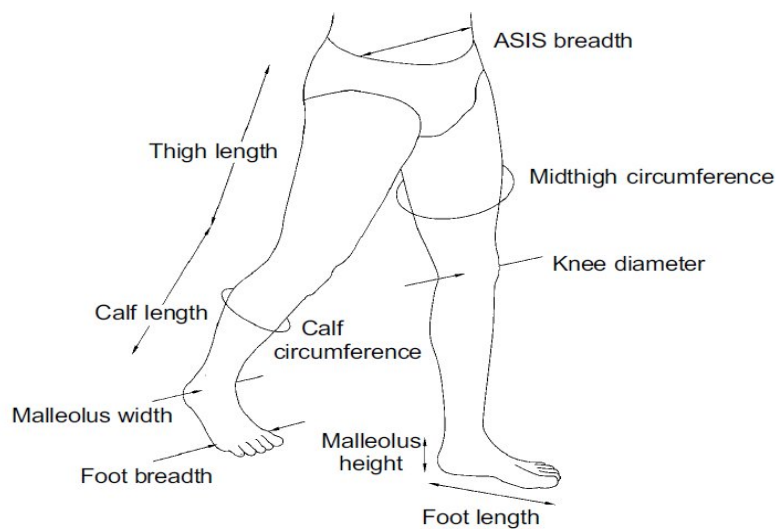


Figure 2.7: Anthropometric measurement that is required in the body segment parameter [11]

2.9 Mass and moment of inertia of segment

2.9.1 Mass of segment

Mass and moment of inertia of body segment can be calculated by using anthropometric measurement data about principle orthogonal axis. The various masses expressions may be presented as

$$\text{Mass of thigh} = (.1032) (\text{total body mass}) + (12.76) (\text{thigh length}) (\text{midthigh circumference})^2 + (-1.023)$$

$$\text{Mass of calf} = (0.0226) (\text{Total body mass}) + (31.33) (\text{Calf length}) (\text{Calf circumference})^2 + (0.016)$$

$$\text{Mass of foot} = (0.0083) (\text{Total body mass}) + (254.5) (\text{Malleolus width}) (\text{Malleolus height}) (\text{Foot length}) + (-0.065)$$

2.9.2 Moment of inertia of segment

Moment of inertia of a segment is the segment resistance to the angular movement and has the unit of (kilogram) (metre)²

$$\text{Segment moment of inertia} = C1 (\text{Total body mass}) (\text{Length})^2 + C2$$

Where C1 and C2 are regression coefficients. One may assume that the shape of thigh and calf is similar to cylinder and foot geometry is similar to the right pyramid as shown in Figure 2.8.

Equation used for estimation of moment of inertia of each segment about principle axis may be presented as.

$$\text{MOI of cylinder about flex/ext axis} = 1/12(\text{mass}) [\text{length}^2 + \text{circumference}^2]$$

$$\text{MOI of cylinder about int/ext axis} = 1/8\pi^2 (\text{mass})(\text{circumference})^2$$

$$\text{MOI of cylinder about abd /add axis} = 1/12(\text{mass}) [\text{length}^2 + \text{circumference}^2]$$

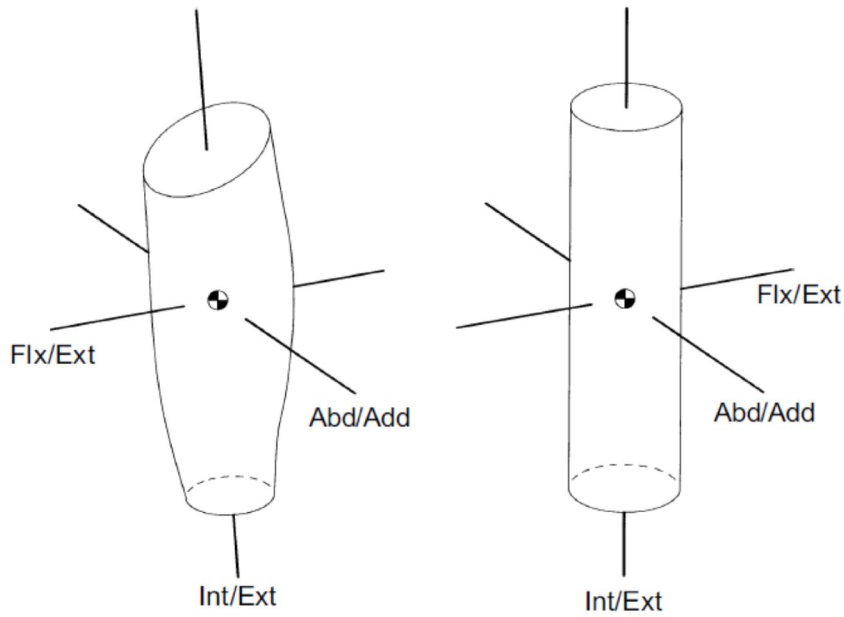


Figure 2.8: thigh is shown in cylinder form with principle orthogonal axis [11]

Table 2.2: Values of each segments anthropometric parameter

Segment Number	1	2	3	4	5	6	7
Segment Name	pelvis	R. thigh	L.thigh	R.calf	L.calf	R.foot	L.foot
Mass(kg)	8.3780	6.86	6.82	3.28	3.28	0.77	0.76
CG position	.56	.39	.39	.42	.42	.44	.44
MOI Flex/ext axis	.01513	.1238	.1257	.0490	.0490	.0035	.0035
MOI Abd/add axis	-	.1188	.1207	.0504	.0504	.0040	.0039
MOI Int/ext axis	-	.0229	.0220	.0037	.0037	.0011	.0011

2.10 Determination of segment orientation

The main task of gait analysis is to obtain segment orientation in 3D plane. This is done by placing a reference system (xyz) in each segment, which will define how a segment oriented relative to the global reference system (XYZ). The location of each reference system is at the segment centre of gravity. As shown in Figure 2.9, XYZ is a global reference system and one may have centre of gravity of each segment (Pelvis, thigh, calf, and foot) has reference system xyz . In the thigh the reference system x runs from distal end to proximal end between knee joint and hip joint as shown in Figure 2.9, xz plane is formed by the hip joint and y axis is orthogonal to xz plane.

For shank reference system, x runs from distal end to proximal end between ankle joint and knee joint as shown in Figure 2.9. Again, xz plane is formed by knee joint and y axis is perpendicular to both axis and pointed to the person's left.

In the case of feet, x axis runs from toe to heel and xy plane is formed at the ankle joint and z axis is also perpendicular to each other and pointed towards person's left as shown in Figure 2.9.

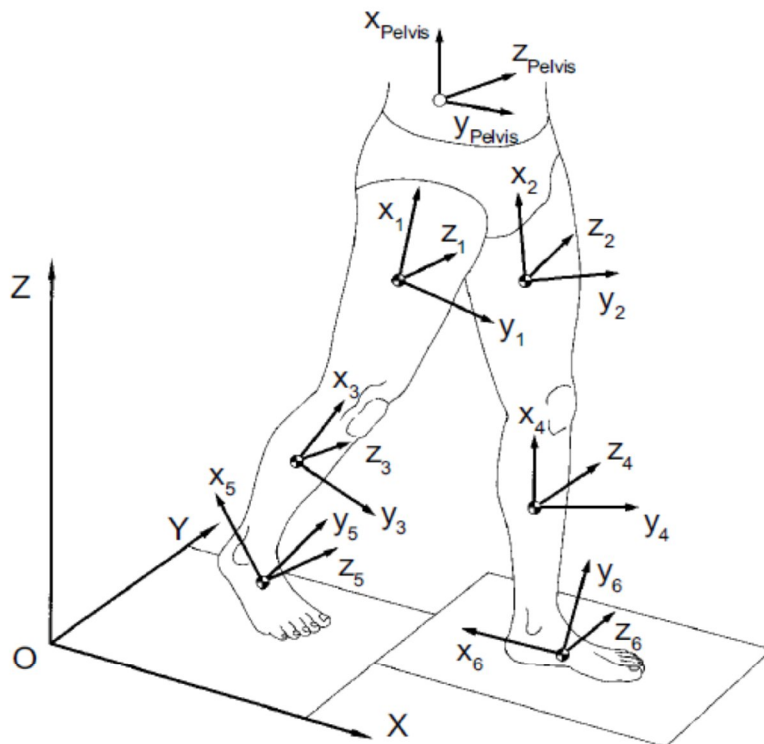


Figure 2.9: Orientation of segment in global coordinate system [11]

2.10.1 Definition of anatomical joint angle

Flexion and extension takes place about the z axis of the proximal segment as shown in Figure 2.9. The internal and external rotation takes place about the longitudinal axis of the segment distal end as x axis shown in the Figure 2.9. However, abduction and adduction takes place about a axis, which is perpendicular to the both flex/ext and int/ext joint angle axis.

Segment joint angle in global coordinate system will be at time 0.00 second provided in table 2.2. When heel strike angle made by each segment with respect to other segment is measured in degree in the gait lab by use of marker system in the lower limb.

Table 2.2 is created in the gait lab of normal male, which has normal height and normal weight about 69 kg. Angle made by each segment of left and right leg provided in table, which shows that all three angles are presented in table. However flex/ext and abd/add angle are used during simulation.

Table 2.2: Segment joint angle in global coordinate system

Segment/joint	Flex/ext(degree)	Abd/add(degree)	Int/ext(degree)
Right thigh/hip	18.9	-5.0	-3.7
Left thigh/hip	-21.8	2.1	-13.3
Right calf/knee	10.4	4.1	-1.7
Left calf/knee	18.9	5.1	9.0
Right foot/ankle	-7.6	-6.8	16.8
Left foot/ankle	-9.7	-8.3	-19.0
Segment/joint	Tilt	Obliquity	Rotation
Pelvis	2.8	8.4	9.2

2.11 Measurement of Ground Reaction Force

As presented earlier, there are two method of analysis of human gait (i) Direct simulation method in which all forces and joint torque are given to the system and by using spring and damper on the foot and ground reaction force is calculated and with the help of ground reaction force one may validate the model (ii) Inverse dynamic simulation technique, which is used to analyse the human gait, in this method all external forces are to be given to the system, in which ground reaction force is the most important force, which act on the foot

during running, walking, and standing. Ground reaction force also helps in balancing the body.

Force plate measurement is used to predict the ground reaction force in the lab. Ground reaction force is generally measured in 3D plane.

- i. Ground reaction force applied in X direction (F_x)
- ii. Ground reaction force applied in vertical direction (F_y)
- iii. Ground reaction force applied in Z direction (F_z)

Generally a common type of force plate measurement instrument is used to measure the force as shown in Figure 2.10. It is a flat plate supported by tri axial transducers. Considering the coordinates of each transducer to be $(0, 0)$, $(0, Z)$, $(X, 0)$, and (X, Z) . The location of the center of pressure is determined by the relative vertical forces at each of these corner transducers.

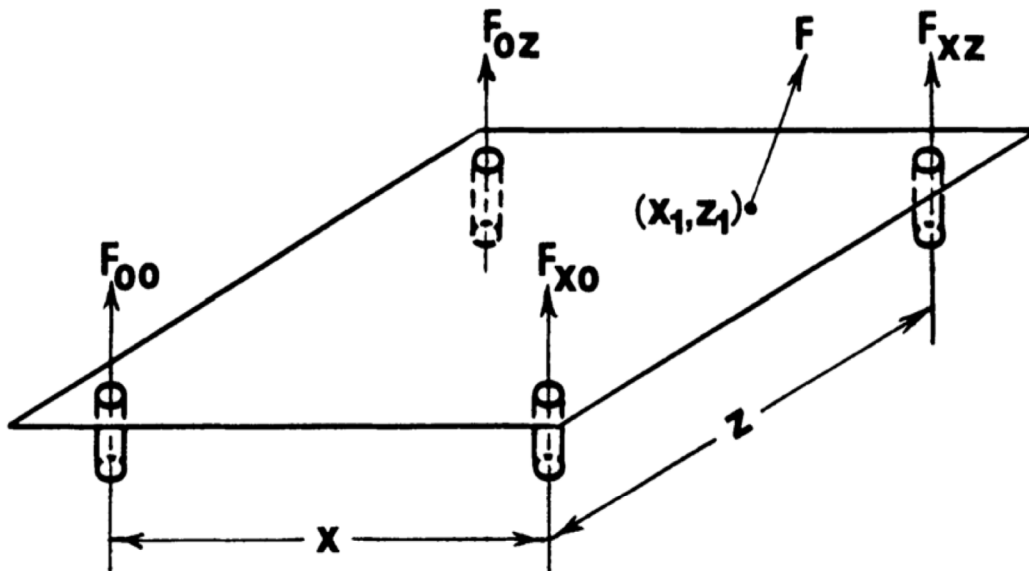


Figure 2.10: Flat force plate measuring instrument

There are several observation and which must be considered while analysing the F_x , F_y and F_z forces. The vertical force is three times greater than the fore-aft force F_x and mediolateral force F_y has the value less than one tenth of vertical force as shown in Figure 2.11

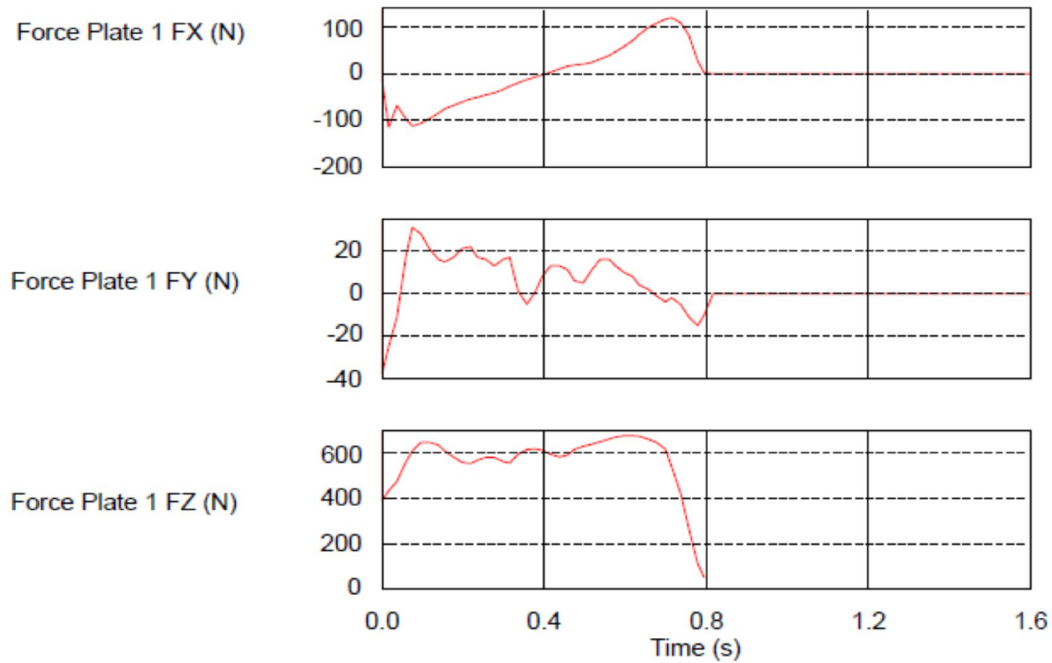


Figure 2.11: Force plate measurement data

2.12 Summary of the chapter

In this chapter one may understand the anthropometric measurement and body segment parameter. Also this chapter includes the forces applied on segment and various body segment parameter involved in analysis of human leg. Ground reaction force generated during normal walking are presented in this chapter. Bond graph modelling has been discussed detail in chapter 3

BOND GRAPH MODELING OF HUMAN LEG

3.1 Introduction

A Bond graph is a graphical representation of a physical dynamic system. It is similar to the better known block diagram and signal-flow graph, with the major difference that the arcs in bond graphs represent bi-directional exchange of physical energy, while those in block diagrams and signal-flow graphs represent uni-directional flow of information. Also, bond graphs are multi-energy domain (e.g. mechanical, electrical, hydraulic, etc) and domain neutral. This means a bond graph can incorporate multiple domains seamlessly.

The bond graph is composed of the "bonds" which link together "single port", "double port" and "multi port" elements. Each bond represents the instantaneous flow of energy (dE/dt) or power. The flow in each bond is denoted by a pair of variables called 'power variables' whose product is the instantaneous power of the bond. For example, the bond of an electrical system would represent the flow of electrical energy and the power variables would be voltage and current, whose product is power. Each domain's power variables are broken into two types: "effort" and "flow". Effort multiplied by flow produces power, thus the term power variables. Every domain has a pair of power variables with a corresponding effort and flow variable. Examples of effort include force, torque, voltage, or pressure; while flow examples include velocity, current, and volumetric flow. The table below contains the most common energy domains and the corresponding "effort" and "flow".

A bond has two other features described briefly here, and discussed in more detail below. One is the "half-arrow" sign convection. This defines the assumed direction of positive energy flow. As with electrical circuit diagrams and free-body diagrams, the choice of positive direction is arbitrary, with the caveat that the analyst must be consistent throughout with the chosen definition. The other feature is the "causal stroke". This is a vertical bar placed on only one end of the bond. It is not arbitrary. As described below, there are rules for assigning the proper causality to a given port, and rules for the precedence among ports. Any port (single, double or multi) attached to the bond shall specify either "effort" or "flow" by its causal stroke, but not both. The port attached to the end of the bond with the "causal stroke" specifies the "flow" of the bond. And the bond imposes "effort" upon

that port. Equivalently, the port on the end without the "causal stroke" imposes "effort" to the bond, while the bond imposes "flow" to that port.

3.2 Power variables

Power is multiplication of two factor effort (e) and flow (f). In multidimensional it is inner, dot, or scalar product of effort and flow which gives the power.

The following Table 3.1 gives the effort and flow variables for the formulation of physical system.

Table 3.1 Effort and flow variable in different systems [18]

System	Effort (e)	Flow (f)
Mechanical	Force	Velocity
	Torque	Angular velocity
Electrical	Voltage	Current
Hydraulic	Pressure	Volume flow rate
Thermal	Temperature	Entropy change rate
	Pressure	Volume change rate
Chemical	Chemical potential	Mass flow rate
	Enthalpy	Mass flow rate
Magnetic	Magnetic motive force	Magnetic flux rate

Here two junctions used one for common effort junction (0) and for common flow junction (1).

3.3 Basic element

Source of effort (SE) element shows the external force associated with the bond, which can be any type of force i.e. in mechanical system. It is a force and torque applied to the system as shown in the Table 3.1.

Source of flow (SF) is the external flow associated with the bond in such a manner that system does not influence the output. In mechanical system, it is velocity and angular velocity as shown in Table 3.1.

Inertial element (I) are mass and inductor is used as conserving element. It is conserved quantity p , which is net accumulating of net effort (e) to the storage element. In Newtonian mechanics, mass does not change with time but in rotary motion inertia varies with time.

Compliant element (C) are used as storing device, which stores all kind of free energy. It is like Hookian springs are an electrical capacitor, which stores energy.

Resistive element (R) is just like Ohm resistance or viscous damper, which is used to dissipate energy.

Transformer element (TF) is like a lever which transforms the energy. So it is like energy transforming element, which receive energy and transform energy with some modulus according to equation. Transformer element transforms energy in the same form i.e. flow to flow and effort to effort.

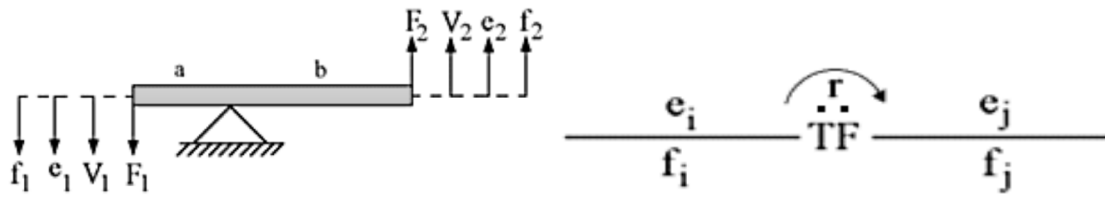


Figure 3.1: A Lever example of transformer and bond graph notation [18]

Gyrator element (GY) is used to transform energy by converting them into some other form i.e., effort to flow and vice versa.

3.4 Causality

Causality established basically cause and effect relationship between the factors of power. In the bond graph, input and output are characterise by casual stroke. It mainly shows the direction of effort.

Table 3.2: Causality of different element

Element	Causality
Inertial element (I)	Towards the element
Compliant element (C)	Toward the junction
Resistance element (R)	Toward both i.e. element and junction
Source of flow (SF)	Toward the element
Source of effort (SE)	Toward the junction
Transformer	Toward the element

3.5 Bond Graph Modeling of rigid beam

Let one may consider a rigid solid in global coordinate system and speed of displacement and rotation of mass centre are independent to one another as shown in Figure 3.2

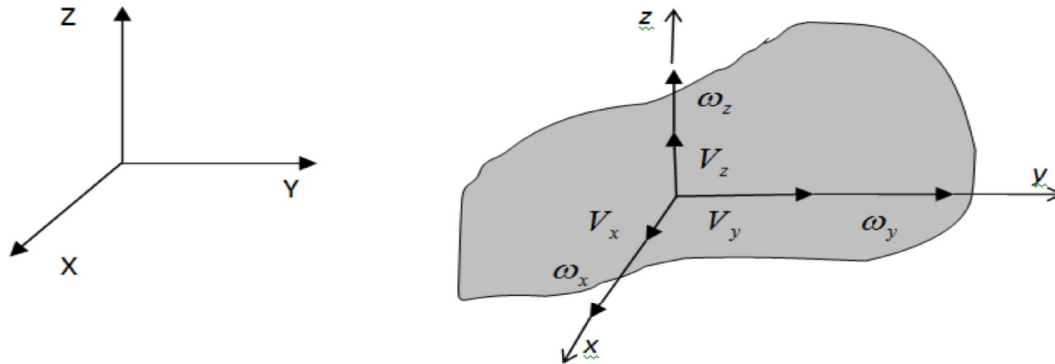


Figure 3.2: Angular velocity and velocity in global coordinate

As shown in Figure 3.3, a rigid beam of mass M and have angular velocity and linear velocity at centre of mass of the beam, is placed in the global coordinate system. The beam has initial velocity \dot{x}_a and \dot{y}_a at the centre of mass.

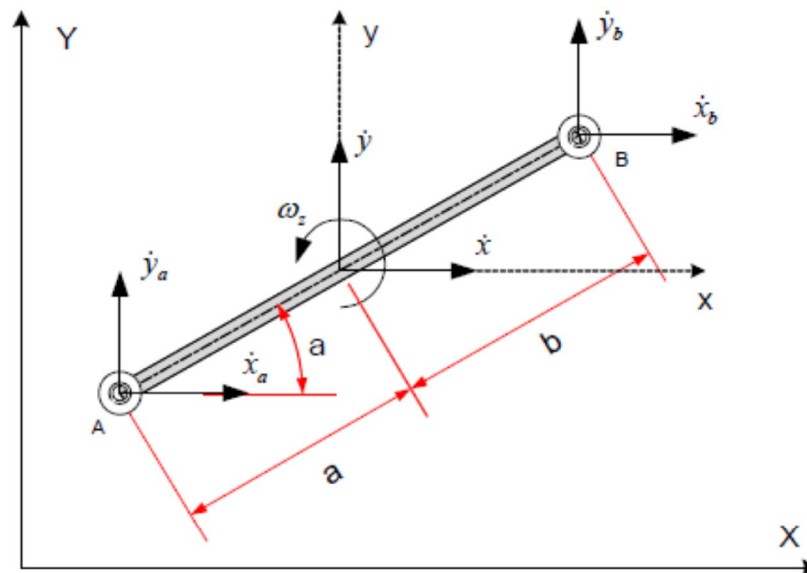


Figure 3.3: Planer 2D rigid beam in global coordinate system

One may deduce velocity at both the end of beam. The following equation may be written as.

$$\dot{x}_a = \dot{x}_c + \omega_z \cdot a \sin\theta \quad (3.1)$$

$$\dot{\theta}_a = -\dot{\theta}_z \cdot a \cos\theta \quad (3.2)$$

$$\dot{\theta}_b = -\dot{\theta}_z \cdot b \sin\theta \quad (3.3)$$

$$\dot{\theta}_b = \dot{\theta}_z \cdot b \cos\theta \quad (3.4)$$

3.5.1 Procedure of modeling single rigid link in global coordinate system

A rigid beam of mass M is in global coordinate system as shown in Figure 3.3. It is supposed that total mass is acting at the centre of mass and beam is rotating with angular velocity $\dot{\theta}_z$. So in the bond graph model of this beam transformer with modulus are used, which mainly act similar to an electrical transformer. It basically transfers effort to effort and flow to flow with some modulus values as shown in Figure 3.1. In the formation of bond graph causality of element must be considered as shown in the Table 3.2. The advantageous feature of the bond graph model is that it automatically remove the causality of system. However, some padding is used to remove the causality. In padding C and R element are used with value (C=.001) and (R=10000). The Figure 3.4 shows the detail bond graph of rigid beam in global coordinate system by using Symbol- Sonata software.

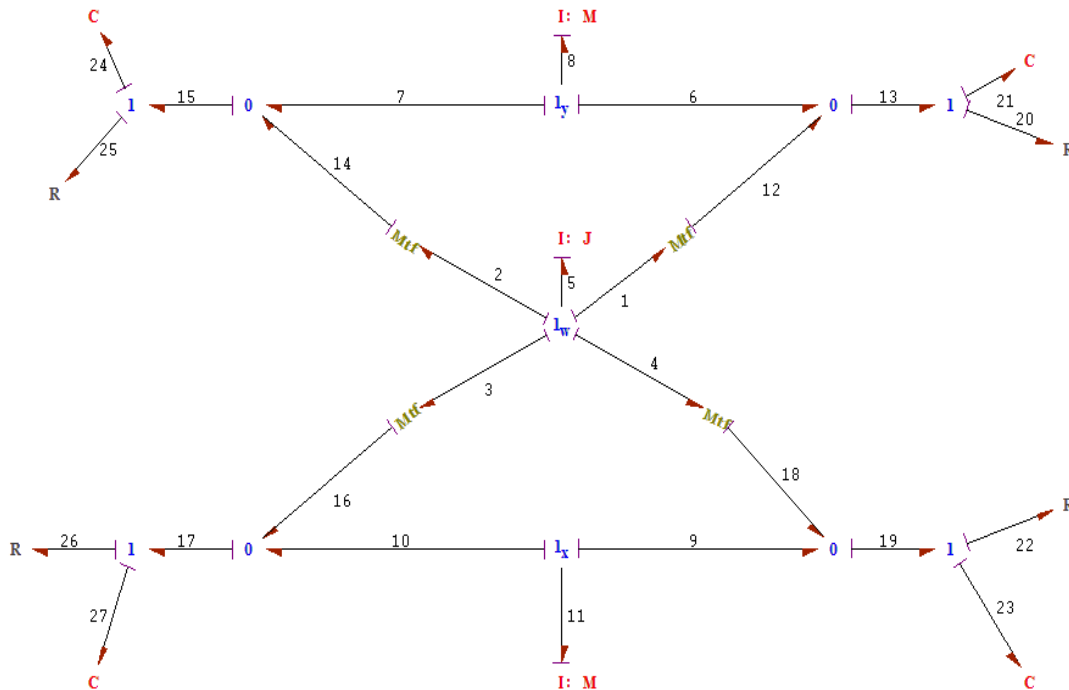


Figure 3.4: Bond graph modelling of rigid beam in global coordinate system

3.5.2 Modeling of two rigid beams with articulated joint

If two rigid beams are connected by an articulated joint. One may create bond graph model using above method which is similar to the modelling of single beam. In this model the joint is having the same velocity. So for common flow, 1 junction is used and for common effort 0 junction is used. Two rigid beams in global coordinate system can be shown in Figure 3.5 are connected by articulated joint and at that junction the velocity is same. Beam 1 has mass M_1 and Beam 2 has mass M_2 , which act at the centre of mass of the segment. Both beams are rotating by angular velocity ω and linear velocity at the COM so velocity at both ends may be deduce out using equation 3.1 to 3.4.

In this model transformer transforms angular velocity into translational velocity at both ends of beam as shown in integrated model of beam, shown in Figure 3.6. In simulation angular velocity is only source of flow input because in human gait initial velocity is considered to be zero. In the transformer modulus, the relation between angle and lever arm may be taken as expressed in Appendix B.

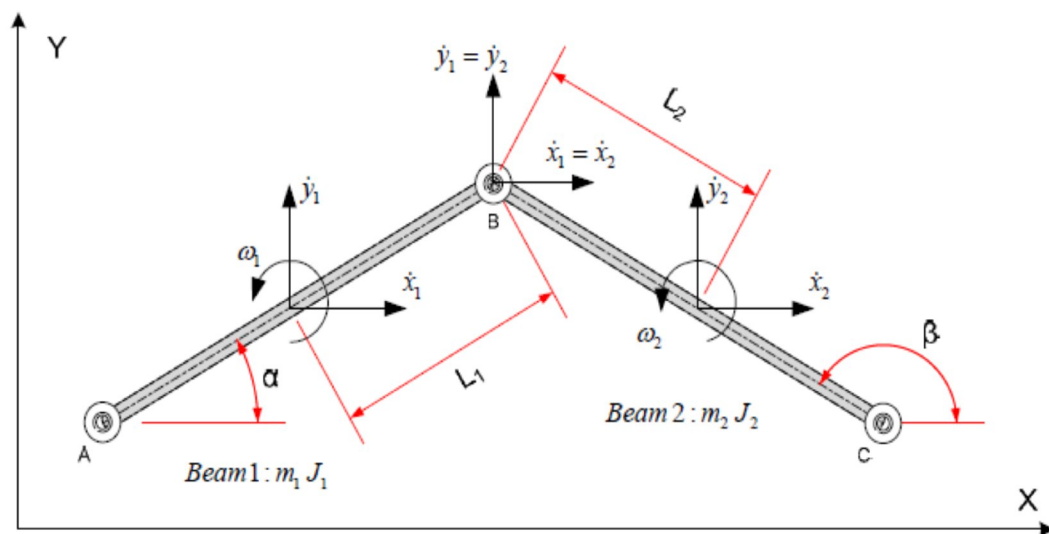


Figure 3.5: Two 2D rigid beam in global coordinate system.

Same procedure has been followed as in the modelling of single rigid beam. However two beam are joined with articulated joint, so as to have same velocity of both beam. In this way, junction 1 (common flow) is used for the joining of beam and transformer element are also used

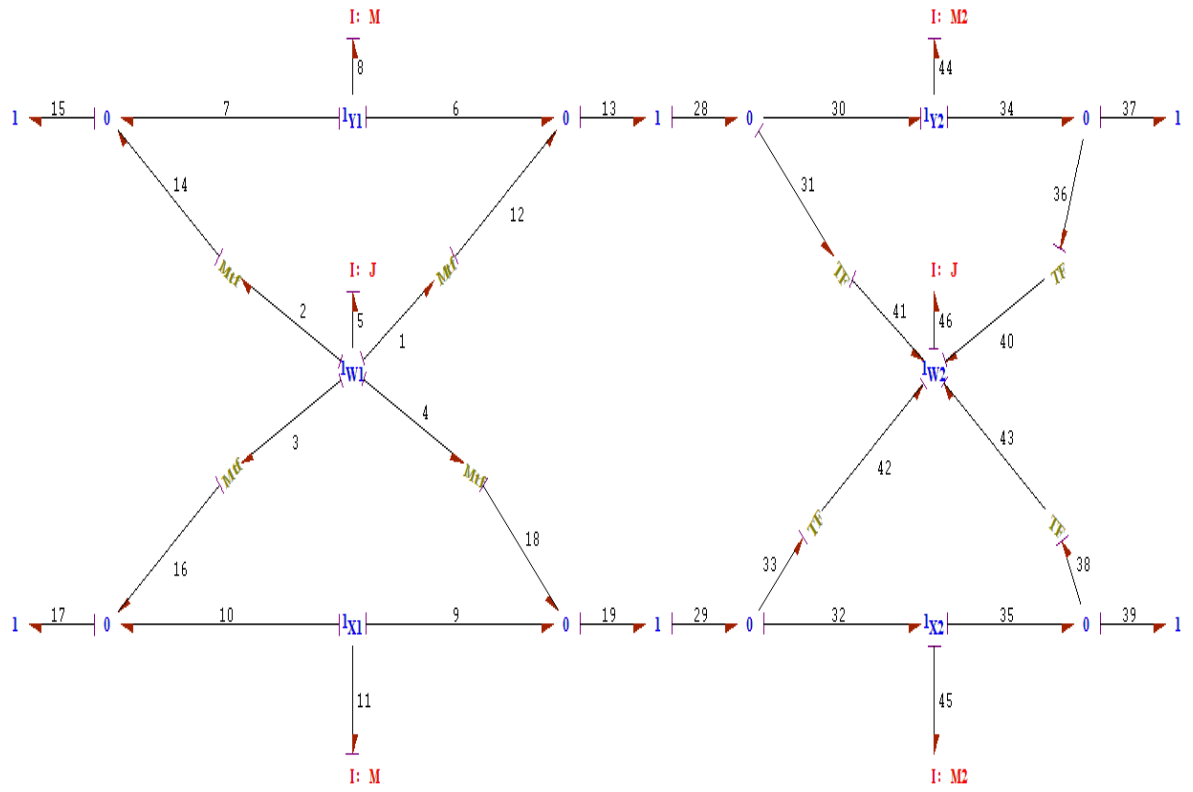


Figure 3.6: Bond graph model of two 2 D rigid articulated beam.

3.5.3 Bond graph of 4 segment model of human leg

In this model 4 segment of right leg which includes pelvis, thigh, calf, feet with articulated joint in 2D XY plane which moves in x and y direction. X is forward and backward direction where as Y is upward and downward direction

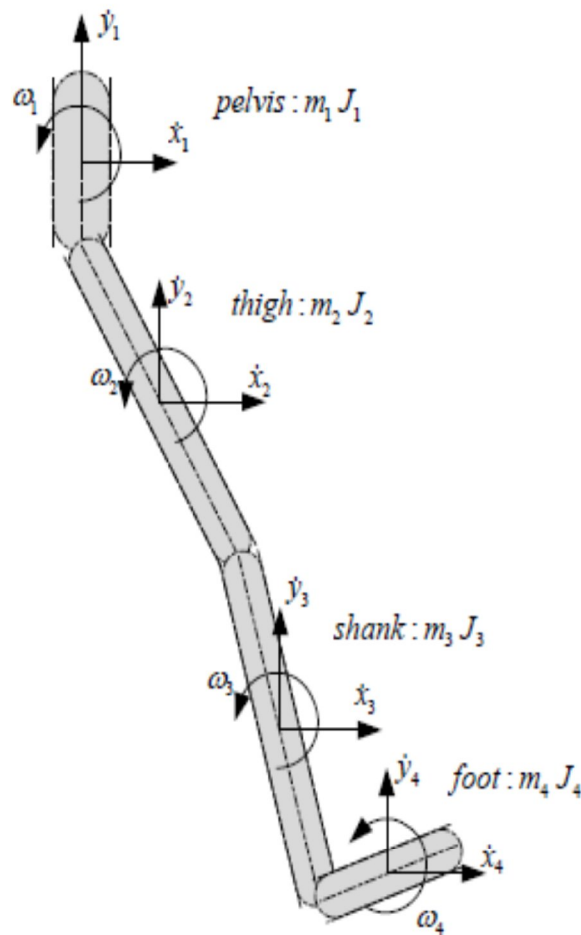


Figure 3.7: Segment models of right leg 1, pelvis, 2 thigh, 3 shank, and 4 foot

In Figure 3.6, shank, thigh and pelvis are connected to each other through articulated joint from down to up foot. At each segment's centre of mass, angular velocity and initial velocity is applied. It is assumed that segment's centre of mass is also centre of gravity which acts vertically downwards. So, gravitational force is also applied at centre of mass. Figure 3.8, shows the integrated bond graph model of system. Angular velocity of each segment is generally function of angular orientation of segment.

3.5.4 Integrated bond graph of right leg 4 segment model of human leg

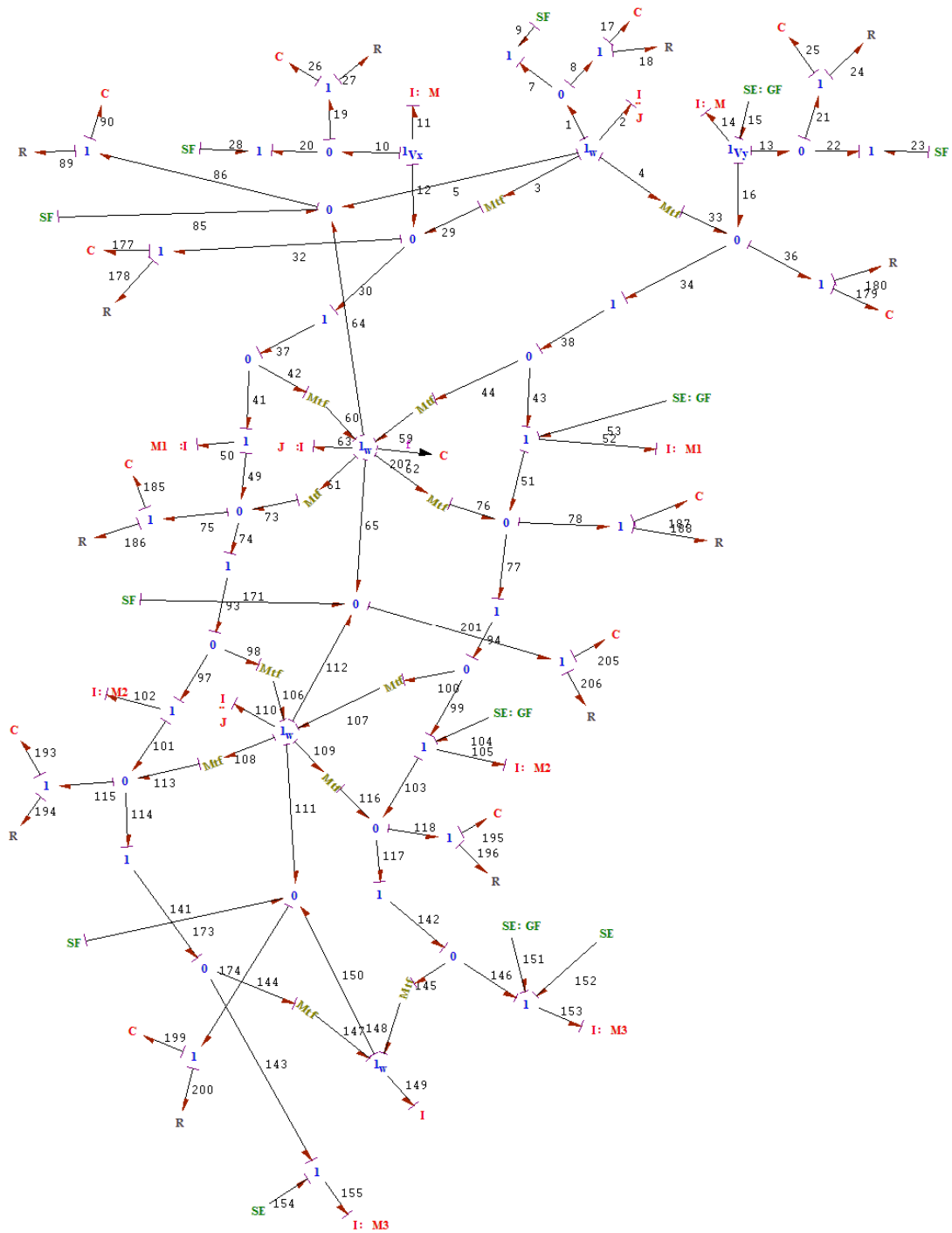


Figure 3.8: Integrated model of 4 segment of human leg.

3.5.5 Bond graph of 7 segment articulated lower limb of human

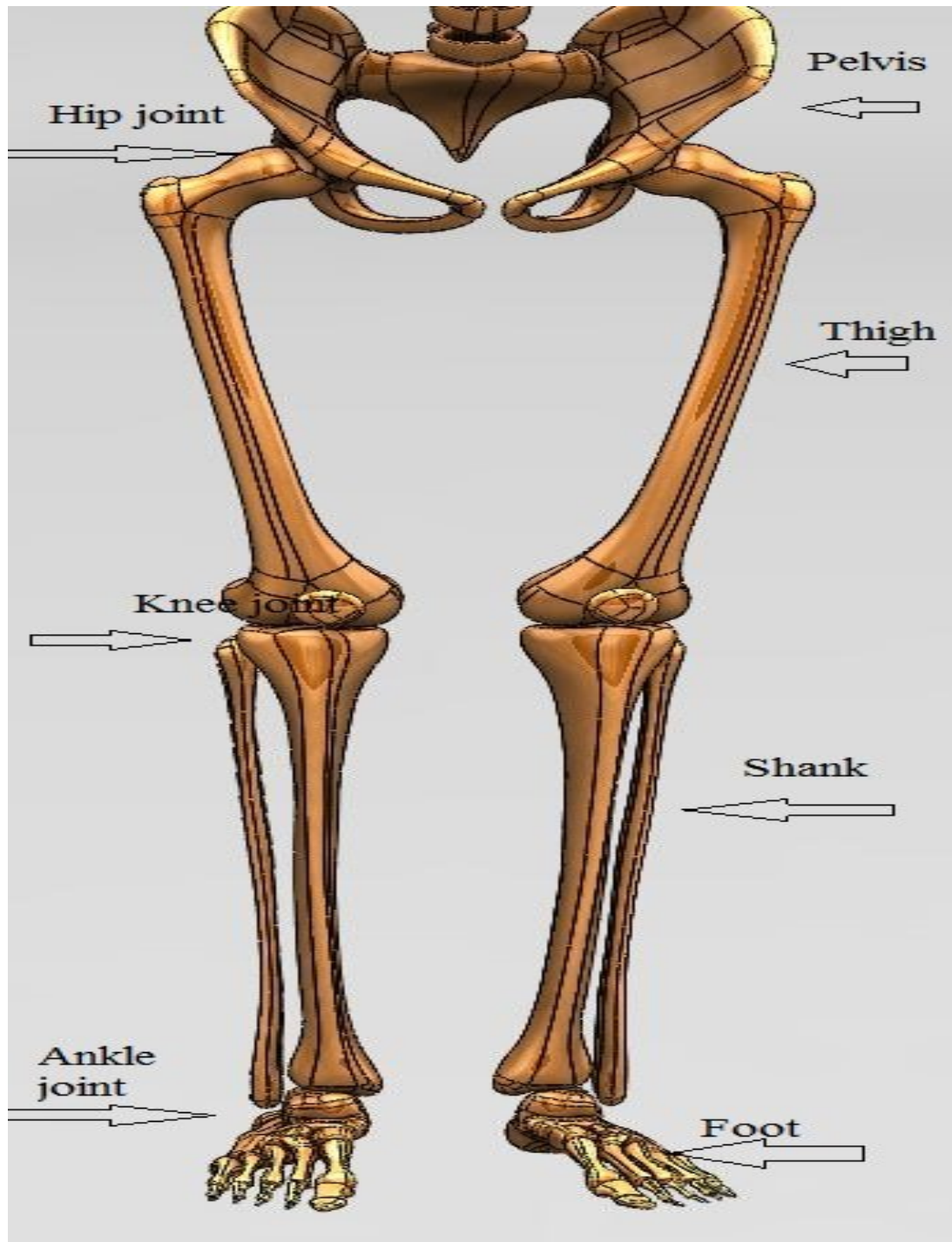


Figure 3.9: Skeleton system of human leg

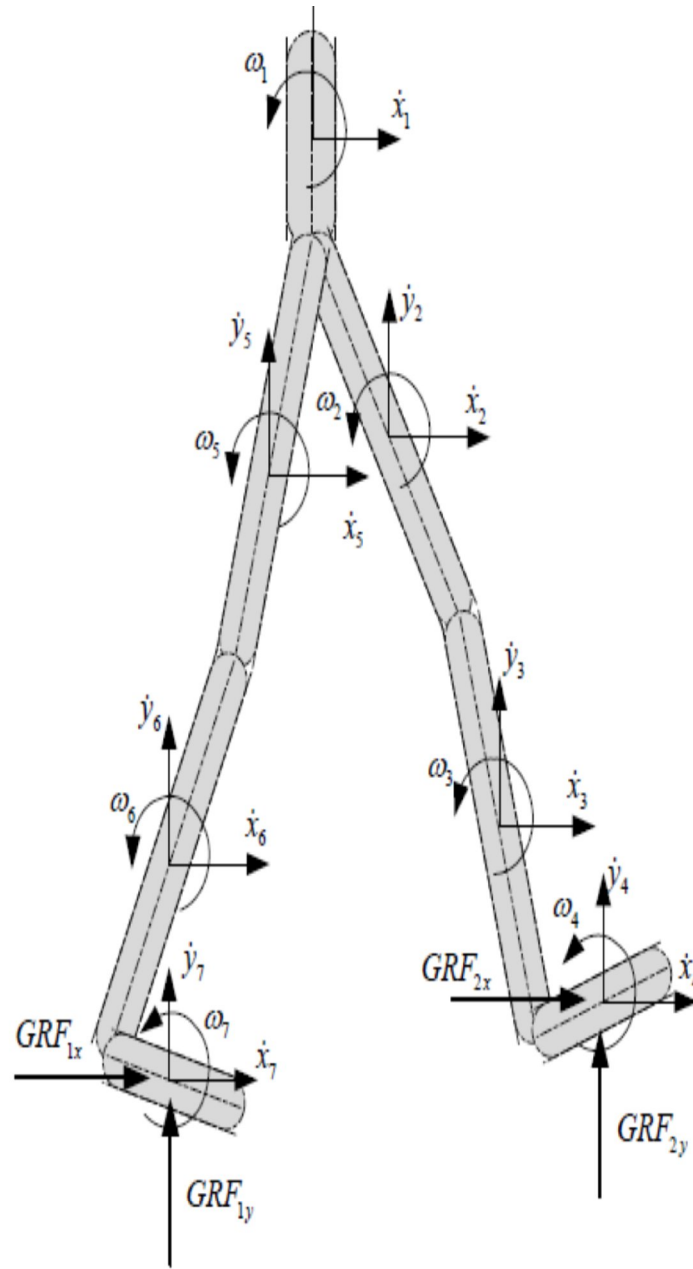


Figure 3.10: Physical model of human lower limb 1-pelvis, 2-5 thigh, 3-6 shank, 4-7 foot.

The skeleton system of human leg is shown in Figure 3.9. For simplification it is assumed that each segment is made of single rigid beam and connected through articulated joint. Ground reaction force is applied both in x and y directions. Gravitational force is applied also in each segment at centre of mass. The physical model of human lower limb has been shown in Figure 3.10.

3.5.6 Integrated bond graph of 7 segment articulated lower limb of human

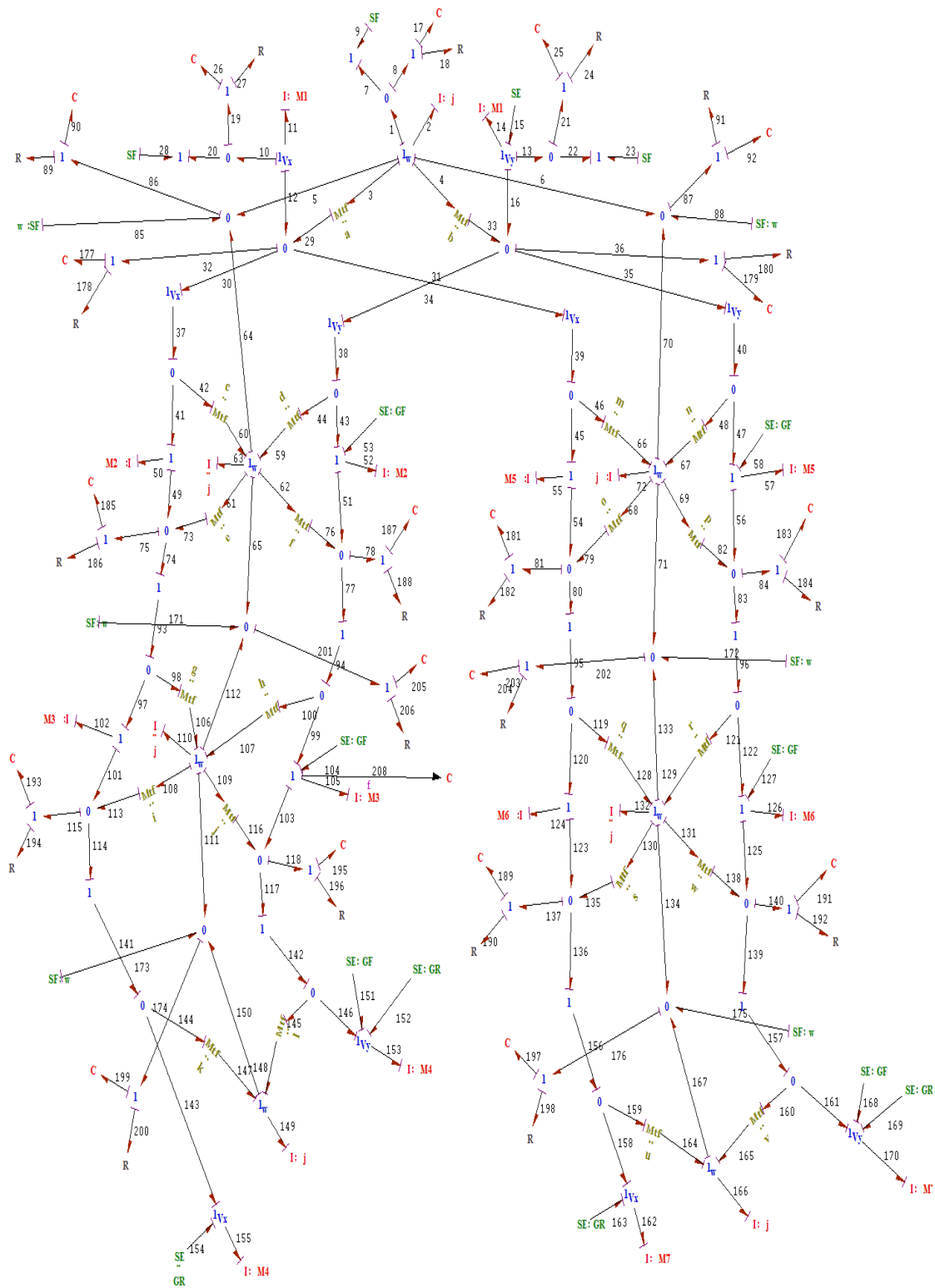


Figure 3.11: Integrated 7 segment model of human leg

Integrated 7 segment model of lower limb is shown in Figure 3.11. Modeling of 7 segment model is done on Symbol Sonata software. Modeling of segments start from pelvis and connected by articulated joint to all other segment as shown in Figure 3.11. Gravitational force and ground reaction force are applied in the model as external source of effort (SE). Angular velocity of segment is applied as external source of flow (SF). To remove causality some padding are used at segment's joint.

3.6 Summary of the chapter

In this chapter basic concept of bond graph modelling and element of symbol sonata software are presented. Modelling procedure applied in modelling of single rigid beam and skeleton model of human leg is discussed in detail. Next chapter deals with dynamic simulation of skeleton model.

4.1 Introduction

Computer simulation can compress the performance of a system over the years into a few minutes of computer running time. Simulation models are comparatively flexible and can be modified to accommodate the changing environment to the real situation. As the complexities of the problem increase the scope of application of simulation equations. In this research, multi-body approach is applied to investigate the dynamic behaviour and modeling of Human leg using Bond Graphs modeling and simulation has been carried out at SYMBOLS-Sonata software.

4.2 Simulation Environment

The Simulator of Symbols Sonata, which is the base post-processing module of SYMBOLS Sonata, is used for the simulation of the human leg for a complete gait cycle.

4.3 Symbols Sonata Software

SYMBOLS Sonata is the next generation of SYMBOLS software (System Modeling by Bond graph Language and Simulation) running in Microsoft Windows 95/98/XP/NT 4.0 environment. It is a modeling, simulation and control systems software for a variety of scientific and engineering applications. Being a powerful research tool, it can help avoid unaffordable, sophisticated fabrications. One may know precisely the response characteristics of the simulated system. A model in SYMBOL'S Sonata may be created using combination of bond graphic elements, block diagram elements in capsulated forms or others capsules. Even model can be created purely using capsules. Sub-model capsules can be imported from the huge capsules library or can even be created by the modeller himself. The pre-cast capsules give modeller a varieties of choice. They can be opened using the bond pad Editor and customized according to the modeller requirements. Modeller may personalize and organize capsules created by them to separate their capsule group from other users.

4.4 Key Features of SYMBOLS Sonata Software are as follows

- Drawing a Bond graph model.
- Augmenting the model by numbering the bonds, assigning power direction.

- Causality, module of 2-port elements, bond activation etc.
- Validation of the Bond graph. Bond graph's integrity is validated after the model is created.
- Creation of non-integrated observers in form of detectors.
- Equations can be generated and displayed on single pallets.
- Creation of expressions.
- Generation of program code.
- Creation of sub-system models henceforth called as Capsules and incorporation of Capsules in a Bond graph model.
- Fault diagnosis.
- Preparing models for simulator and control modules.
- Export of sub-system and system models to MAT lab/Simulink environment.
- Integrated simulation environment.
- Easy to access control panels.
- Multiple and intelligent entry mode.
- Online plotting, pause, stop and resume option.
- Online parameter variation through slider during simulation.
- Continuous run simulation, multiple simulations of different systems at the same time.
- Simulation extension facility.
- Advance post simulation plotting facilities.
- Online code editing and compilation.
- Different integration methods for stiff equations.
- Multi-run facility with interpolated or discrete parameter values.
- Event handlers and notification messages.
- Direct debugging and variable tracking.
- Improved external data and chart interpolation routines.

4.5 Simulation Properties

The bond graph model of the human leg is simulated for 1.129 sec to obtain different output responses. Total 1024 records are used in the simulation and error is kept in the order of 5.0×10^{-2} . Runge-Kutta Gill method of fifth order is used in present work to solve the differential equations.

4.6 Runge-Kutta Gill method

Runge-Kutte Gill methods propagate a solution over an interval by combining the information from several Euler-style steps (each involving one evaluation of the state equations), and then using the information obtained to match a Taylor series expansion up to some higher order. This method treats every step in a sequence of steps in identical manner. Fifth-order Runge-Kutte method is used in present simulation work

4.7 Parameter Used In Simulation

The normal male weight is considered 69.0 kg and 170 cm height. All data has been adopted by using anthropometric measurement and angular data has been taken from gait lab [11]

Table 4.1: various parameter used in simulation

Parameter	Value	Units
Pelvis length	.7140	M
Pelvis mass	8.3780	Kg
Pelvis moment of inertia(flex/ext)	.01533	Kg m ²
Pelvis angle	2.8	Degree
Right thigh length	.460	M
Right thigh mass	6.86	Kg
Right thigh MOI (flex/ext) axis	.1238	Kg m ²
Right Hip joint angle (flex/ext)axis	+18.9	Degree
Right calf length	.430	M
Right calf mass	3.28	Kg
Right leg MOI (flex/ext)	.0490	Kg m ²
Knee angle(flex/ext)	10.4	Degree
Right Foot length	.260	M
Right foot mass	.77	Kg
Right foot MOI	.0011	Kg m ²
Ankle joint angle	-6.3	Degree

Left thigh length	.465	M
Left thigh mass	6.82	Kg
Left thigh MOI (flex/ext)	.1257	Kg m ²
Left hip joint angle	-21.8	Degree
Left calf length	.430	M
Left calf mass	3.28	Kg
Left leg MOI (flex/ext)	.0490	Kg m ²
Left knee joint angle	18.9	Degree
Left foot length	.260	M
Left foot mass	.76	Kg
Left foot MOI	.0011	Kg m ²
Left ankle joint angle	-8.3	Degree
GRF on right foot in x direction	118	N
GRF on right foot in y direction	645	N
GRF on left foot in x direction	-15	N
GRF on left foot in y direction	271	N

*The angle used in simulation are ext/flex in hip joint, ext/flex in knee joint and abd/add in ankle joint.

4.8 Force generated in the lower segment

In normal walking, when heel strike to the ground the opposite forces (ground reaction force) are applied to the foot in horizontal and vertical direction. It is to be considered that the vertical ground reaction force is four times greater than horizontal ground reaction force. So, the generated force is also greater than the horizontal force as shown various Figs from 4.1 to 4.12.

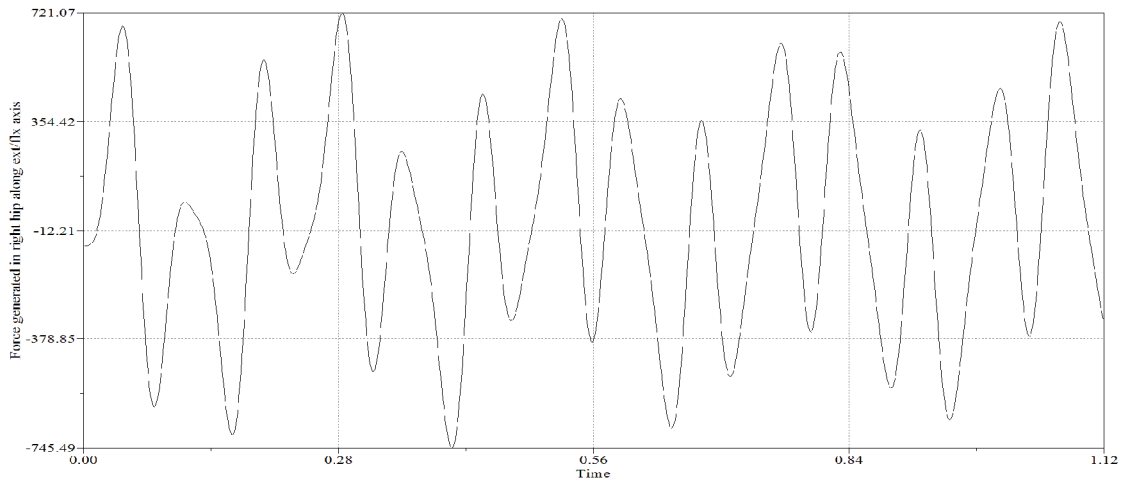


Figure 4.1: Force generated in the right hip along vertical direction (N)

The force generated in the right hip has maximum values 745.49 N (opposite direction), which is greater than the vertical ground reaction force (645 N) applied on the right foot. As soon as the heel strike to the ground, the force starts from extension and continuously increasing towards flexion and at the toe off position, flexion force again reaches maximum value as shown in Figure 4.1.

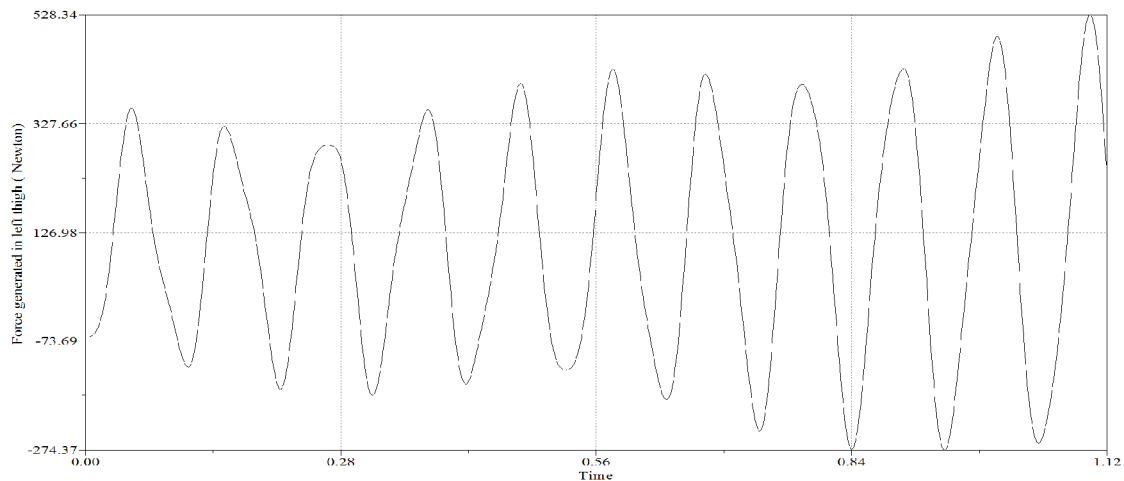


Figure 4.2: Force generated in left hip along vertical direction (N)

As compare to the right hip the force generated in the left hip is less due to the ground reaction force applied on the left leg, which comes to 271 N. In this case the maximum force generated in the left hip is 528.34 N in flexion.

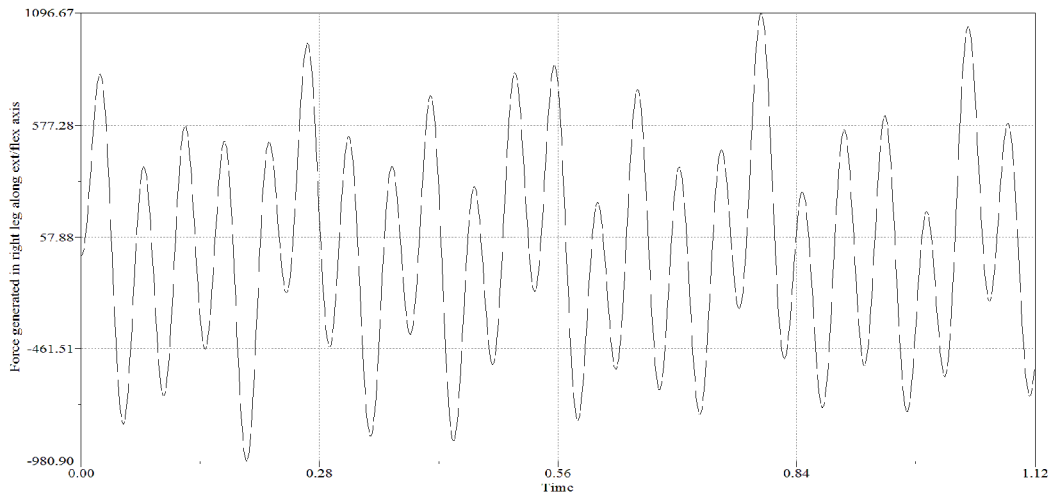


Figure 4.3: Force generated in the right leg along vertical direction (N)

Force generated in the clavicles is much greater than hip force, and has maximum values 1096.67 N in flexion at the starting of swing phase (in swing phase flexion muscle activate) as shown in Figure 4.3.

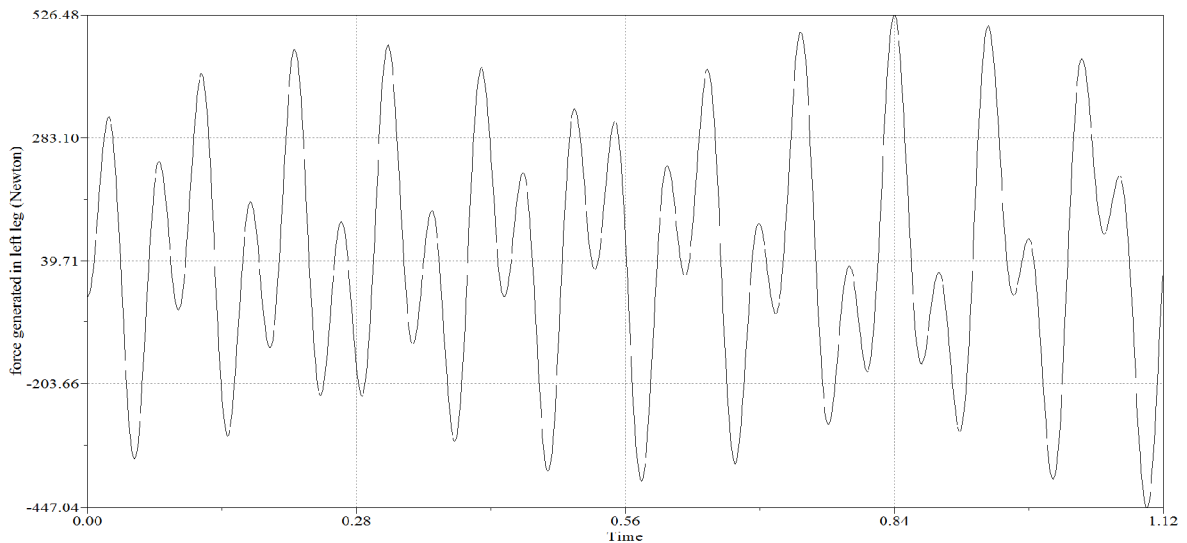


Figure 4.4: Force generated in left leg along vertical direction (N)

Initially left leg is in stationary position i.e. or there is no movement in the left leg. The function of left leg is started when the right leg ends stance phase and start swing phase. In

that case the body weight shifted to the left leg. The maximum force at the left leg in flexion comes out to be 526.48 N as shown in Figure 4.4.

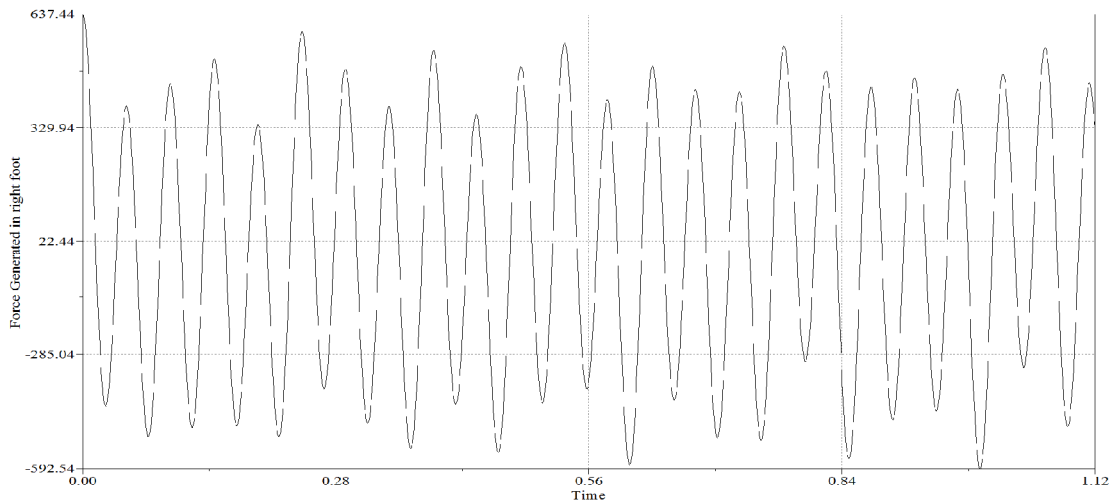


Figure 4.5: Force generated in right foot along vertical direction (N)

Force generated in right foot has maximum value 637.44 N in flexion. It decreases in extension. When one ends stance phase and starts swing phase it has average minimum values about 400 N as shown in Figure 4.5.

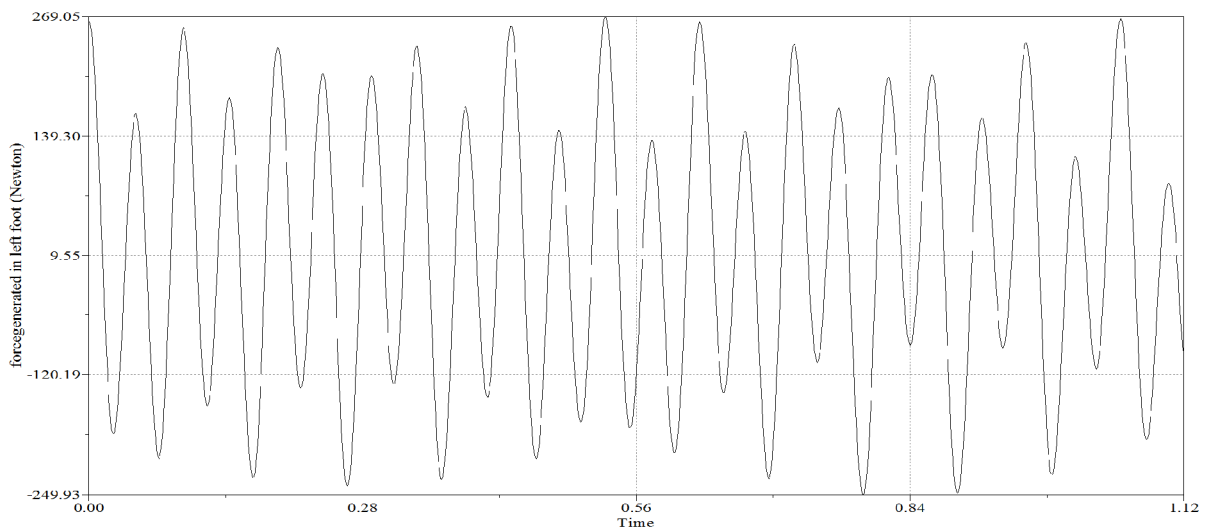


Figure 4.6: Force generated in left foot along vertical direction (N)

Initially, when left foot is on ground then force has value about 269.05 N and when right leg strike to the ground (heel strike), then force starts decreasing and has the same values as in initial conditions, when right foot in swing phase.

4.8 Force generated in the lower segment in horizontal direction

Ground reaction force in horizontal direction is evaluated in simulation as external force applied in the foot. So there is a horizontal force generated in each segment as shown in the Figures 4.7 to 4.12. The initial value of ground reaction force in the horizontal direction is 118 N in right leg and -15 N in left leg as shown in Table 4.1.

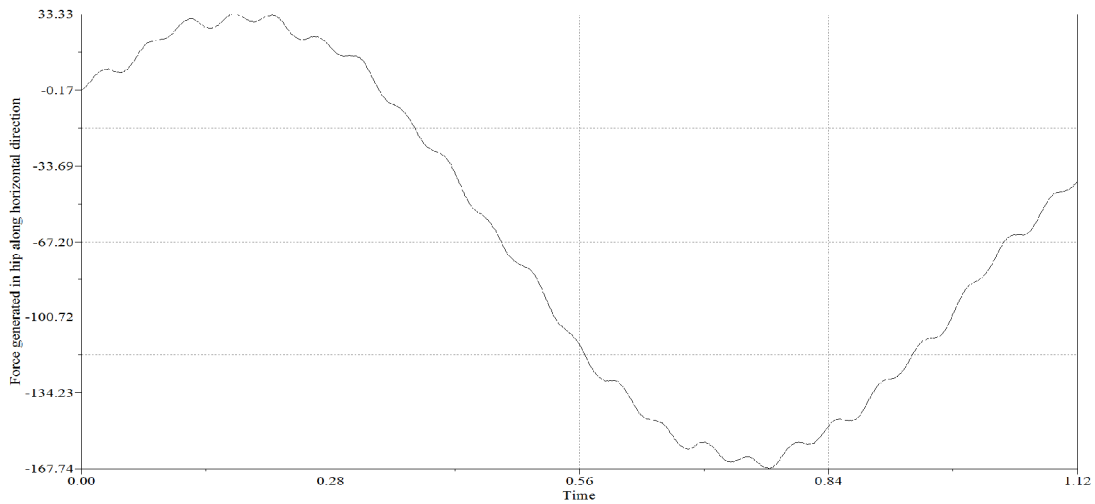


Figure 4.7: Force generated in right hip along horizontal direction (N)

When heel strike, horizontal force applied in forward direction, which starts from -0.17 N and gains the maximum value of 33.33 N in forward direction. As soon as toe off phase began, foot start to accelerate and backward direction force increases continuously and gains maximum value about 167.74 N (opposite direction) as shown in Figure 4.7.

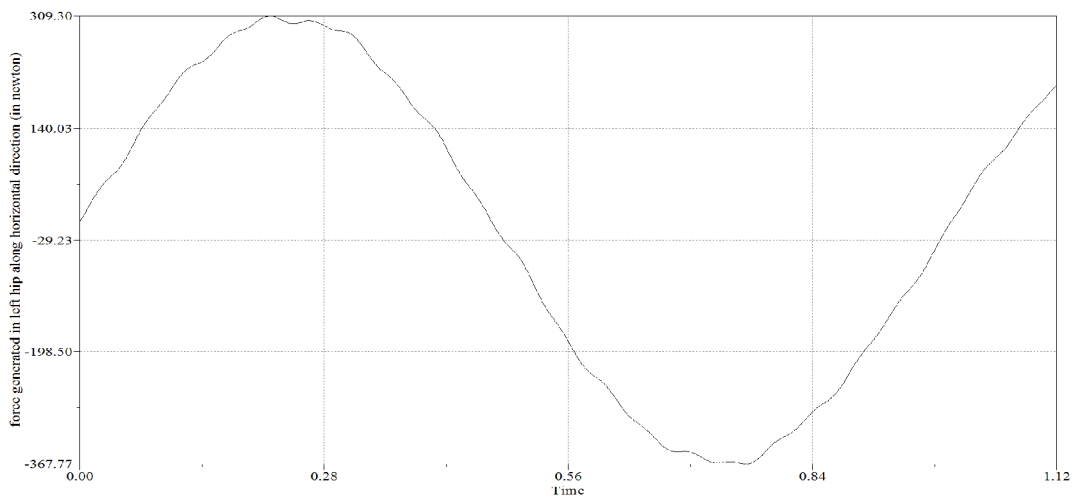


Figure 4.8: Force generated in left hip along horizontal direction (N)

In left hip horizontal force has a large value as compared to right hip. In left hip it attain a maximum value about 367.77 N in opposite direction as shown in Figure 4.8.

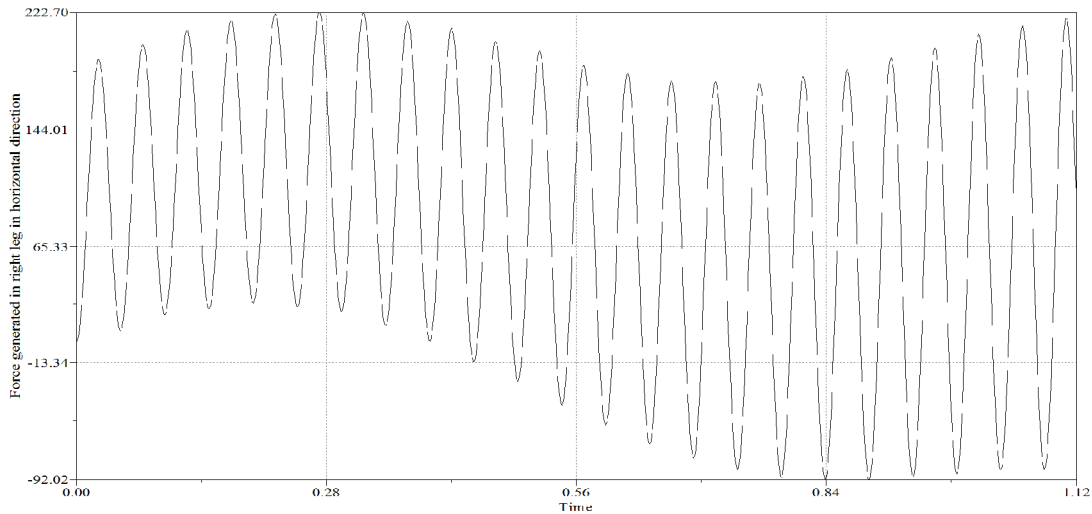


Figure 4.9: Force generated in right leg along horizontal direction (N)

Horizontal force values in right shank varied between +222.70 N to -92.02 N. Positive value is in forward direction and negative values in backward direction as shown in figure 4.9. As soon as heel strike force applied in forward direction, it continuously increases in the forward direction till swing phase starts.

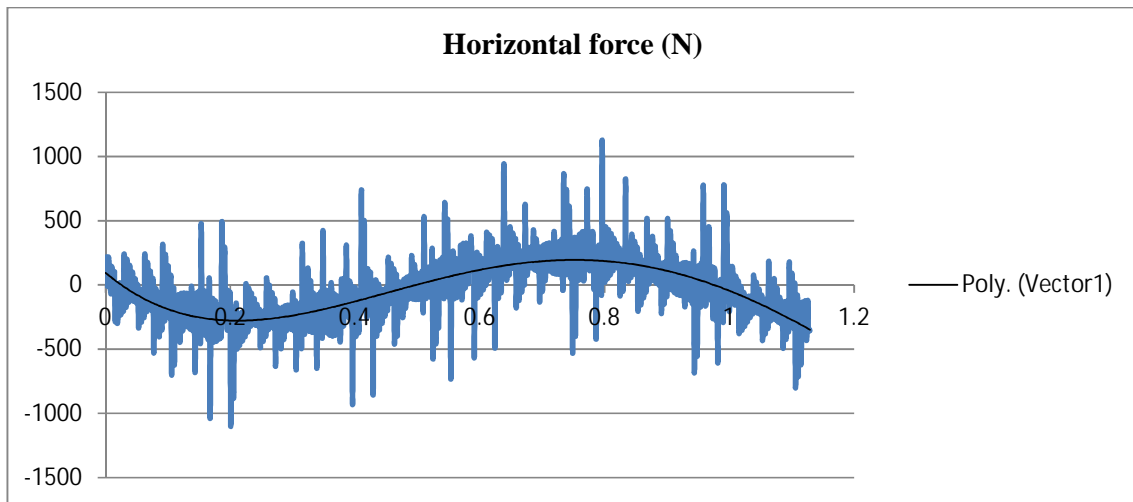


Figure 4.10: Force generated in left shank along horizontal direction (N)

In left shanks horizontal force fluctuate between + 897.17 to – 1073.55 N, as shown in Figure 4.10. It attains maximum value, when right leg in swing position between time period 0.56 second to 0.90 second.

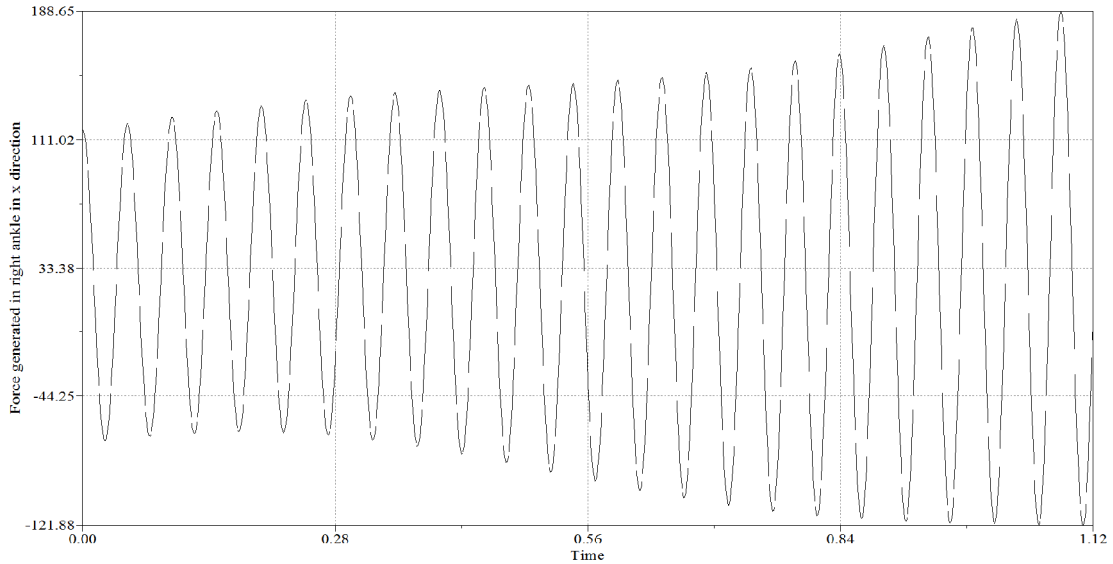


Figure 4.11: force generated in right foot along horizontal direction (N)

In right foot, force generated along horizontal direction varies between 188.65 to 121.88 N (opposite direction), as shown in Figure 4.11. It gains maximum value in the swing phase from 0.84 second to 1.129 second.

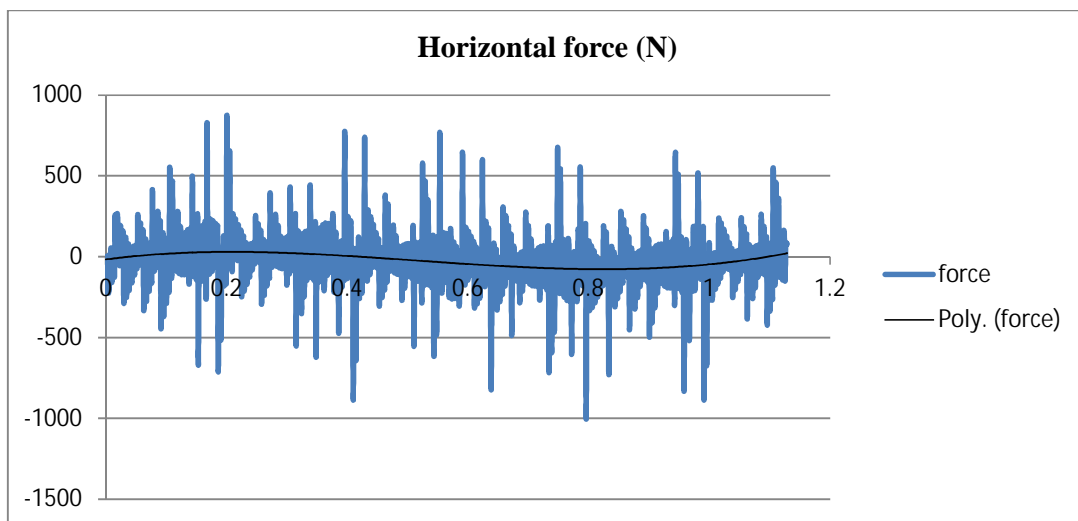


Figure 4.12: Force generated in left foot along horizontal direction (N)

As shown in Figure 4.12, force generated in left foot varies between +858.59 N to -875.98 N.

4.9 Summary of the chapter

In this chapter dynamic simulation of human leg has been introduced and various simulated forces on leg are shown. Here two type of ground reaction forces are considered vertical and horizontal. So in the dynamic simulation vertical and horizontal forces on each segment are discussed.

The torque generated in each segment is not directly simulated by bond graph modelling. One may deduce effort and calculate the moment generated in each segments. Here one complete cycle is equal to the 1.129 second. Henceforth, percentage of cycle is converted in time and one may efficiently time in horizontal axis instead of percentage cycle.

Table 5.1: conversion of complete one cycle into time

	Musculoskeletal model	Human
Walking speed (m/s)	1.28±0.04	1.27±0.11
Step length (m)	.80±0.07	.67±0.06
Stride time (s)	1.125±0.004	1.04±0.10

In this way time is divided into the percentage cycle.

5.1 Torque generated in segment

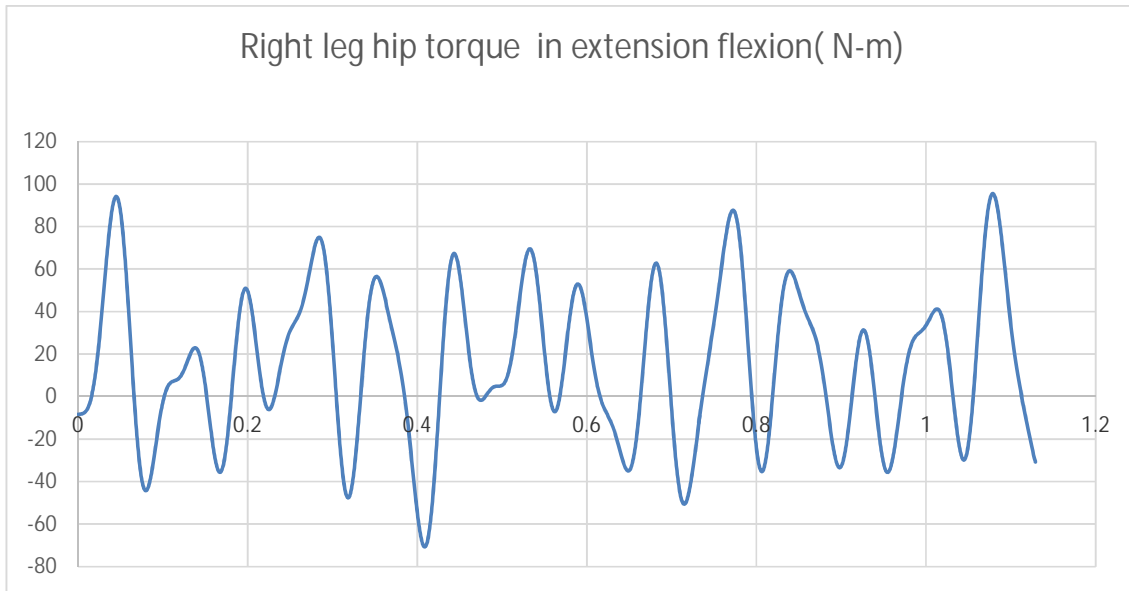


Figure 5.1: Torque generated in right hip due to vertical ground reaction force (N-m)

As shown in Figure 5.1 torque generated in the right hip has the maximum flexion (+ 90 N-m) and extension (-55 N-m). As heel strike to the ground the positive flexion takes place and at the time 0.4 second (midstance), it has maximum extension torque generated and during the time 0.7 to 0.8 second, initial swings starts and the leg is accelerated. Afterward activation of hip flexor muscle occurs and which slowly decelerate the leg and prepare for the next heel strike.

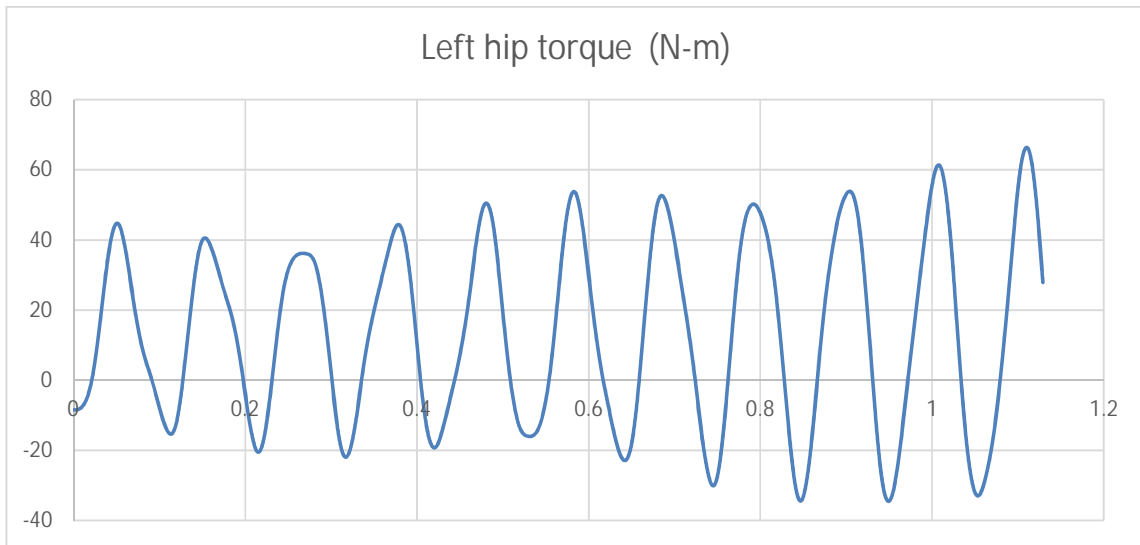


Figure 5.2: Torque generated in left hip in flexion/extension direction (N-m)

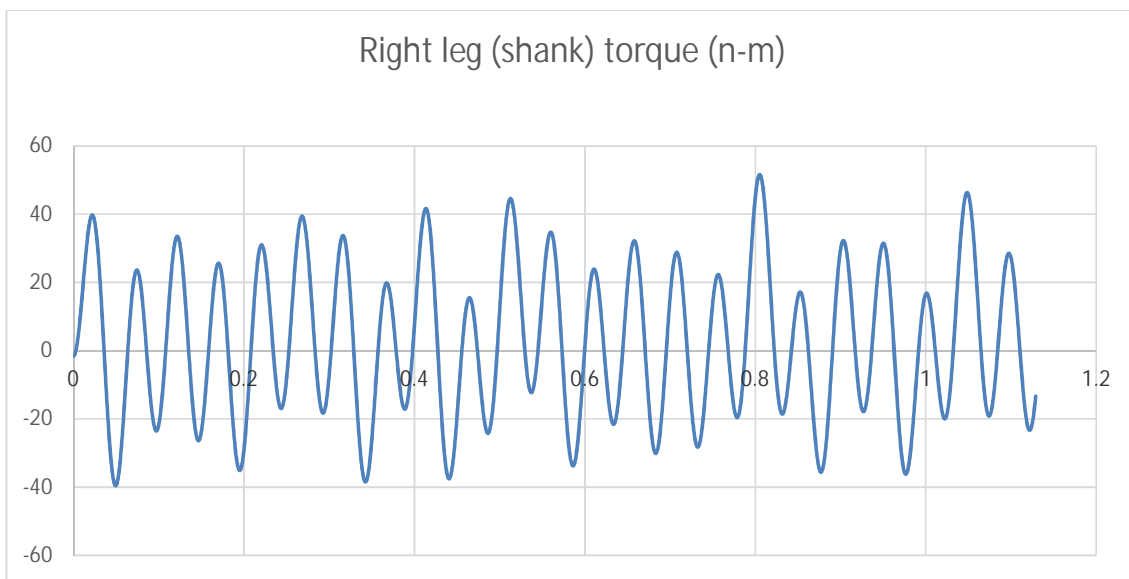


Figure 5.3: Torque generated in right shanks in flexion extension direction (N-m)

As shown in Figure 5.3, the torque generated in the right shanks has the maximum flexion about (50 N-m) and maximum extension torque is about (40 N-m). Whenever heel strike to ground, shank flexion torque is about (40 N-m) and gains maximum extension torque. Calve has maximum flexion torque about (50 N-m) as the foot is in swing position and during this time flexion muscles activated.

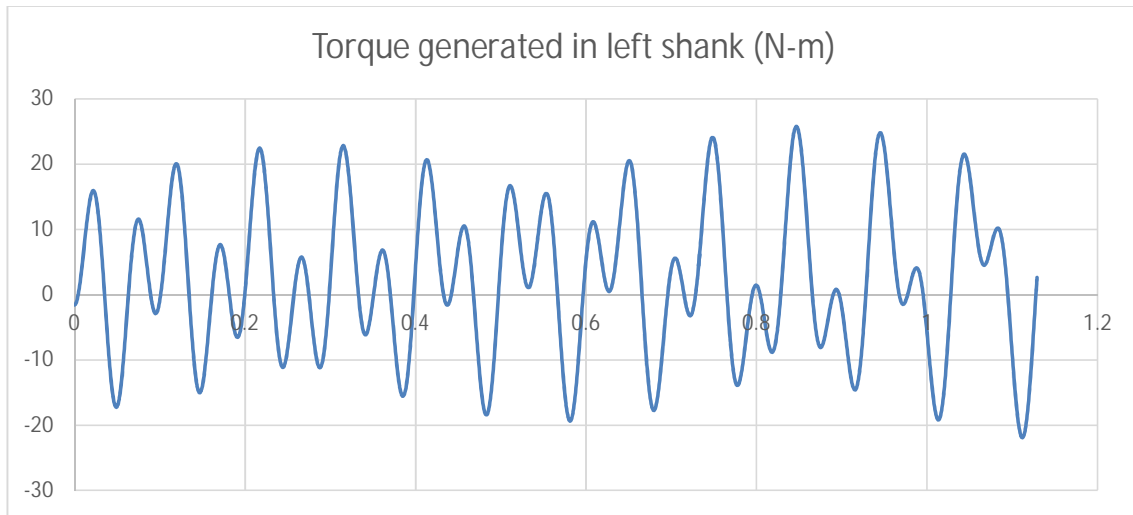


Figure 5.4: Torque generated in left shank in flexion extension (N-m)

As shown in Figure 5.4, the torque generated in the left shanks has the maximum flexion moment about 35 N-m whenever left heel strike and right leg swing phase start. At the time of right leg heel strike it has very less torque about 15 N-m.

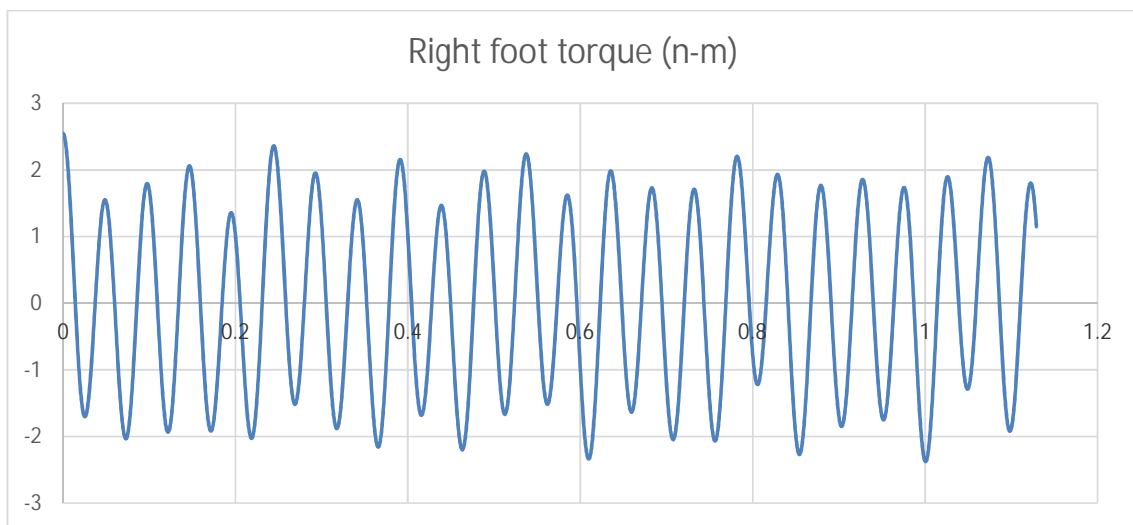


Figure 5.5: Torque generated in right foot in flexion extension (N-m)

In right foot, torque generated varies between ± 3 N-m as shown in Figure 5.5. It starts from the value $+ 3$ N-m and varies between ± 2 N-m as shown in Figure 5.5.

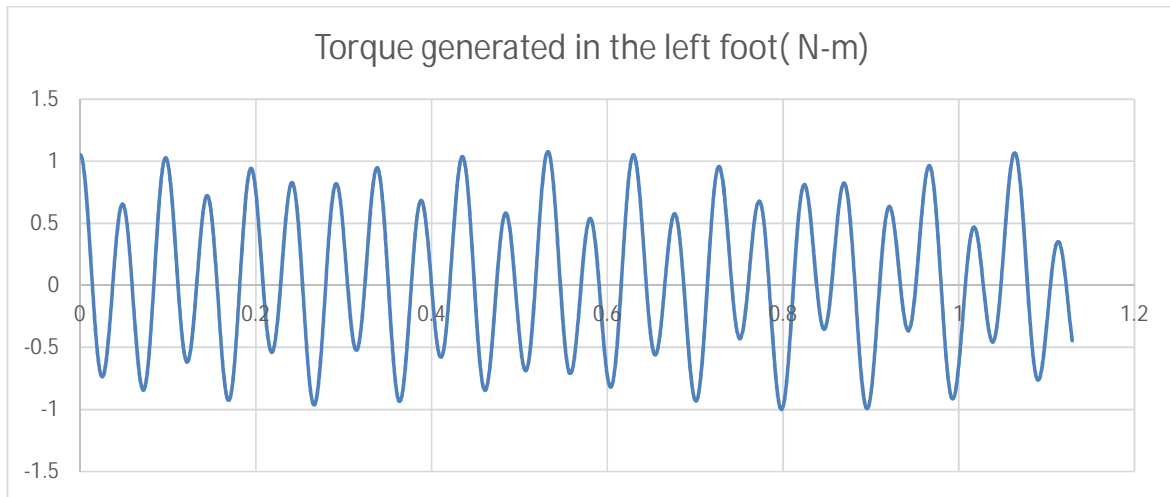


Figure 5.6: Torque generated in left foot in flexion extension (N-m)

As shown in Figure 5.6, the torque generated in left foot initially starts from the value 1 N-m because left foot is static on the ground whenever right leg heel strike occurs. Afterwards its value varies between ± 1 N-m.

5.2 Generated moment about centre of mass

In bond graph model one may introduce moment of inertia at the centre of mass which provides us angular momentum, which may be expressed as

$$\Sigma \text{Moment} = \text{rate of change of angular momentum}$$

So the moments generated in the right leg (thigh, shank and foot) are clearly shown in Figure 5.7 to Figure 5.9.

Maximum flexion moment in thigh is 11.07 N-m and maximum extension moment is 10.74 N-m as shown in the Figure 5.7. Rate change of angular momentum starts from 0.16 N-m and increases in extension moment afterward flexion moment takes place about 10 N-m. As the foot is in swing phase, rate change of angular momentum reaches maximum value about 11.07 N-m.

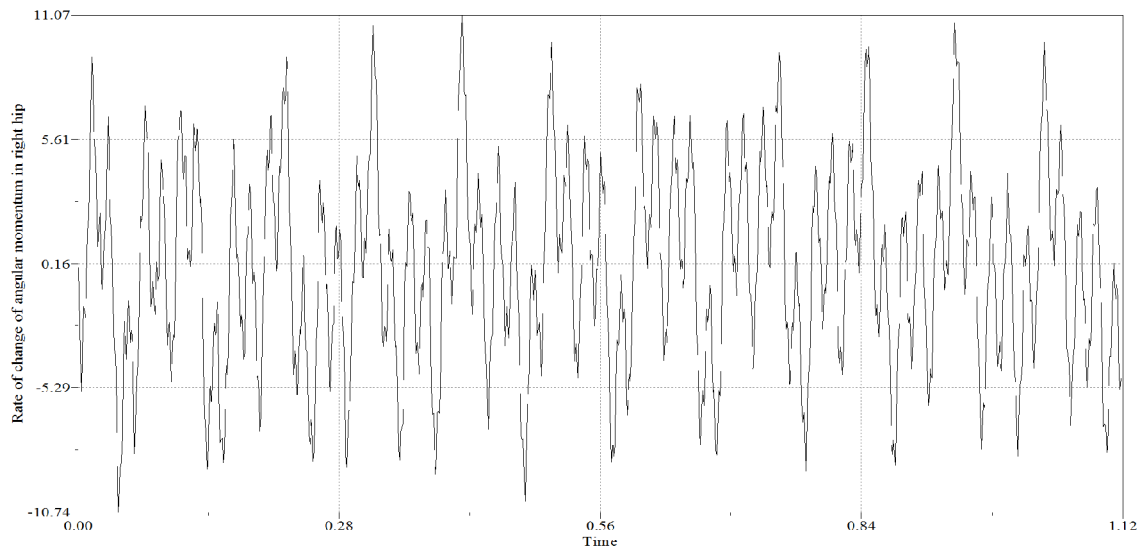


Figure 5.7: Moment in right hip (N-m)

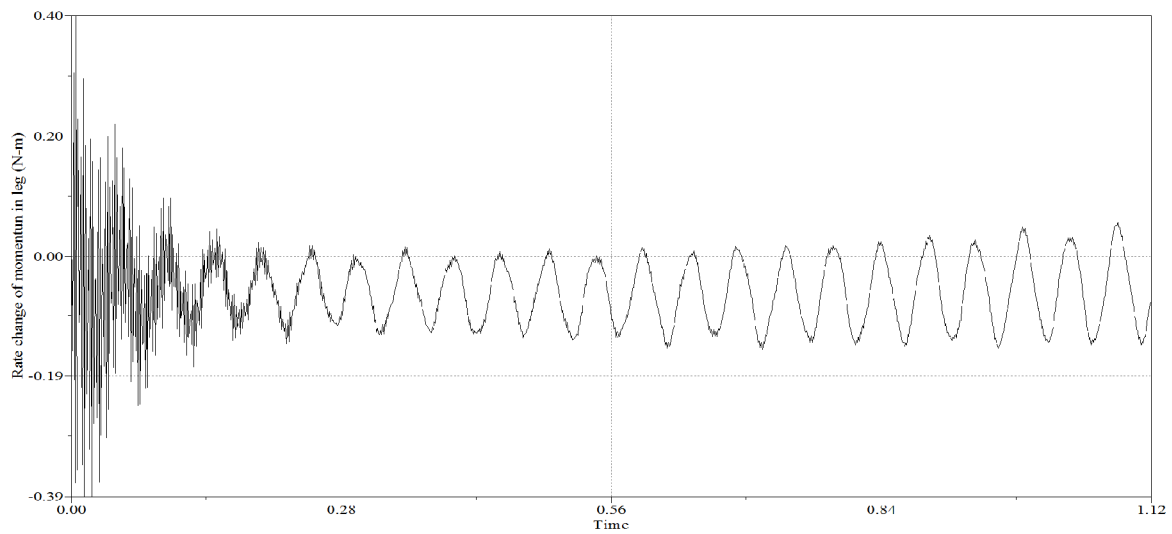


Figure 5.8: Moment in left calve (N-m)

As shown in Figure 5.8 flexion moment generated in the shank is 0.40 N-m and extension moment 0.39 N-m. Rate change of angular momentum in shank is mainly about time 0.20 second. Afterward shank has almost constant value as shown in Figure 5.8. One may see in Figure 5.8, rate change of angular momentum is very less as compared to thigh because the orientation of segment is comparatively very less.

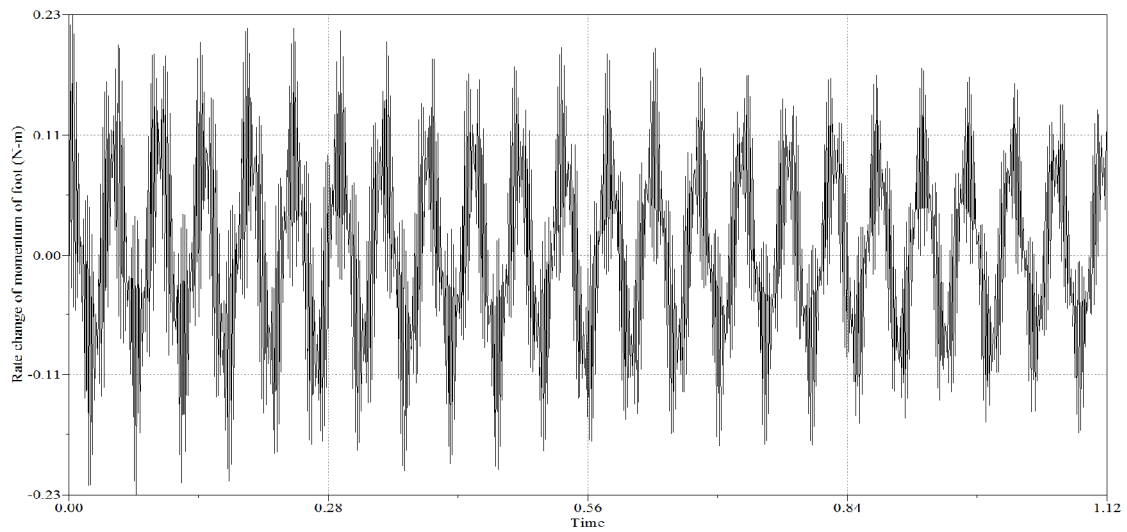


Figure 5.9: Moment in right foot. (N-m)

Moment generated in right foot varies between ± 0.23 N-m. Initially start from 0.00 N-m and gains maximum moment about 0.23 N-m in flexion as shown in Figure 5.9. Rate change of angular momentum in foot is very less as compared to thigh and shank because angular orientation of thigh is much greater than angular orientation of foot as seen in Table 2.2.

Chapter 6

Conclusions and future scope

6.1 Conclusions

This dissertation work has been attempted to obtain the dynamic behaviour of human leg through bond graph technique and to evaluate the various forces acting on the leg through computer simulation.

Two dimensional skeleton model of human leg is constructed by using bond graph technique and simulated, for dynamic simulation. One may easily conclude that the modeling and simulation result gives matching result with archival literature. The force generated in segment due to the ground reaction force applied on the system and torque generated in the segment is also analysed. There are may be marginal error in the results due to non considerations of muscle force in the model and each segment considered as the single rigid beam, whereas thigh is a single rigid bone, in actual. However shank and foot are made with several bones and their flexibility must be accounted in the simulation parameter

6.2 Future scope

In future the model may be improved by following way

1. By Adding muscle force to the model.
2. By using some low level controller in the model.
3. Bond graph modeling of system in 3D plane.

Please note: 'd' represents the time derivative of the state variable within the first parenthesis.

$$\begin{aligned}
 d(P110) &= 1/g*(K185*Q185+R186*(P50/M50+e*P63/M63-P102/M102- \\
 &\quad 1/g*P110/M110))+h*(K187 \\
 &\quad *Q187+R188*(P52/M52+f*P63/M63-P105/M105-h*P110/M110))- \\
 &\quad i*(K193*Q193+R194 \\
 &\quad *(i*P110/M110+P102/M102-P155/M155-k*P149/M149))- \\
 &\quad j*(K195*Q195+R196*(j*P110 \\
 &\quad /M110+P105/M105-l*P149/M149-P153/M153))-K199*Q199- \\
 &\quad R200*(SF173+P110/M110 \\
 &\quad +P149/M149)-K205*Q205-R206*(SF171+P110/M110+P63/M63) \\
 d(P105) &= K187*Q187+R188*(P52/M52+f*P63/M63-P105/M105-h*P110/M110)- \\
 &\quad K195*Q195-R196 \\
 &\quad *(j*P110/M110+P105/M105-l*P149/M149-P153/M153)+SE104 \\
 d(P102) &= K185*Q185+R186*(P50/M50+e*P63/M63-P102/M102-1/g*P110/M110)- \\
 &\quad K193*Q193-R194 \\
 &\quad *(i*P110/M110+P102/M102-P155/M155-k*P149/M149) \\
 d(P132) &= 1/q*(K181*Q181+R182*(P55/M55+o*P72/M72-1/q*P132/M132- \\
 &\quad P124/M124))+r*(K183 \\
 &\quad *Q183+R184*(P57/M57+p*P72/M72-r*P132/M132-P126/M126))- \\
 &\quad s*(K189*Q189+R190 \\
 &\quad *(P124/M124+s*P132/M132-P162/M162-1/u*P166/M166))- \\
 &\quad w*(K191*Q191+R192*(P126 \\
 &\quad /M126+w*P132/M132-v*P166/M166-P170/M170))-K203*Q203- \\
 &\quad R204*(SF172+P72/M72 \\
 &\quad +P132/M132)-K197*Q197-R198*(SF175+P132/M132+P166/M166) \\
 d(P126) &= K183*Q183+R184*(P57/M57+p*P72/M72-r*P132/M132-P126/M126)- \\
 &\quad K191*Q191-R192 \\
 &\quad *(P126/M126+w*P132/M132-v*P166/M166-P170/M170)+SE127 \\
 d(P124) &= K181*Q181+R182*(P55/M55+o*P72/M72-1/q*P132/M132-P124/M124)- \\
 &\quad K189*Q189-R190
 \end{aligned}$$

$$*(P124/M124+s*P132/M132-P162/M162-1/u*P166/M166)$$

$$d(P72)= 1/m*(K177*Q177+R178*(a*P2/M2+P11/M11-P50/M50-1/c*P63/M63-P55/M55-1/m*P72/M72))+n*(K179*Q179+R180*(b*P2/M2+P14/M14-P52/M52-d*P63/M63-P57/M57-n*P72/M72))-o*(K181*Q181+R182*(P55/M55+o*P72/M72-1/q*P132/M132-P124/M124))-p*(K183*Q183+R184*(P57/M57+p*P72/M72-r*P132/M132-P126/M126))-R91*(P2/M2+SF88+P72/M72)-K92*Q92-K203*Q203-R204*(SF172+P72/M72+P132/M132)$$

$$d(P57)= K179*Q179+R180*(b*P2/M2+P14/M14-P52/M52-d*P63/M63-P57/M57-n*P72/M72)-K183*Q183-R184*(P57/M57+p*P72/M72-r*P132/M132-P126/M126)+SE58$$

$$d(P55)= K177*Q177+R178*(a*P2/M2+P11/M11-P50/M50-1/c*P63/M63-P55/M55-1/m*P72/M72)-K181*Q181-R182*(P55/M55+o*P72/M72-1/q*P132/M132-P124/M124)$$

$$d(P63)= d*(K179*Q179+R180*(b*P2/M2+P14/M14-P52/M52-d*P63/M63-P57/M57-n*P72/M72))+1/c*(K177*Q177+R178*(a*P2/M2+P11/M11-P50/M50-1/c*P63/M63-P55/M55-1/m*P72/M72))-e*(K185*Q185+R186*(P50/M50+e*P63/M63-P102/M102-1/g*P110/M110))-f*(K187*Q187+R188*(P52/M52+f*P63/M63-P105/M105-h*P110/M110))-R89*(P2/M2+SF85+P63/M63)-K90*Q90-K205*Q205-R206*(SF171+P110/M110+P63/M63)$$

$$d(P52)= K179*Q179+R180*(b*P2/M2+P14/M14-P52/M52-d*P63/M63-P57/M57-n*P72/M72)-K187*Q187-R188*(P52/M52+f*P63/M63-P105/M105-h*P110/M110)+SE53$$

$$d(P50)= K177*Q177+R178*(a*P2/M2+P11/M11-P50/M50-1/c*P63/M63-P55/M55-1/m*P72/M72)-K185*Q185-R186*(P50/M50+e*P63/M63-P102/M102-1/g*P110/M110)$$

$$d(P155)= K193*Q193+R194*(i*P110/M110+P102/M102-P155/M155-$$

$$k * P149 / M149 + SE154$$

$$d(P149) = k * (K193 * Q193 + R194 * (i * P110 / M110 + P102 / M102 - P155 / M155 - k * P149 / M149)) + l * (K195 * Q195 + R196 * (j * P110 / M110 + P105 / M105 - l * P149 / M149 - P153 / M153)) - K199 * Q199 - R200 * (SF173 + P110 / M110 + P149 / M149)$$

$$d(P153) = K195 * Q195 + R196 * (j * P110 / M110 + P105 / M105 - l * P149 / M149 - P153 / M153) + SE151 + SE152$$

$$d(P162) = K189 * Q189 + R190 * (P124 / M124 + s * P132 / M132 - P162 / M162 - 1 / u * P166 / M166) + SE163$$

$$d(P166) = 1 / u * (K189 * Q189 + R190 * (P124 / M124 + s * P132 / M132 - P162 / M162 - 1 / u * P166 / M166)) + v * (K191 * Q191 + R192 * (P126 / M126 + w * P132 / M132 - v * P166 / M166 - P170 / M170)) - K197 * Q197 - R198 * (SF175 + P132 / M132 + P166 / M166)$$

$$d(P170) = K191 * Q191 + R192 * (P126 / M126 + w * P132 / M132 - v * P166 / M166 - P170 / M170) + SE168 + SE169$$

$$d(P11) = -K26 * Q26 - R27 * (P11 / M11 - SF28) - K177 * Q177 - R178 * (a * P2 / M2 + P11 / M11 - P50 / M50 - 1 / c * P63 / M63 - P55 / M55 - 1 / m * P72 / M72)$$

$$d(P14) = -R24 * (P14 / M14 - SF23) - K25 * Q25 + SE15 - K179 * Q179 - R180 * (b * P2 / M2 + P14 / M14 - P52 / M52 - d * P63 / M63 - P57 / M57 - n * P72 / M72)$$

$$d(P2) = -K17 * Q17 - R18 * (P2 / M2 - SF9) - a * (K177 * Q177 + R178 * (a * P2 / M2 + P11 / M11 - P50 / M50 - 1 / c * P63 / M63 - P55 / M55 - 1 / m * P72 / M72)) - b * (K179 * Q179 + R180 * (b * P2 / M2 + P14 / M14 - P52 / M52 - d * P63 / M63 - P57 / M57 - n * P72 / M72)) - R89 * (P2 / M2 + SF85 + P63 / M63) - K90 * Q90 - R91 * (P2 / M2 + SF88 + P72 / M72) - K92 * Q92$$

$$d(Q205) = SF171 + P110 / M110 + P63 / M63$$

$$d(Q203) = SF172 + P72 / M72 + P132 / M132$$

$$d(Q191) = P126/M126 + w * P132/M132 - v * P166/M166 - P170/M170$$

$$d(Q189) = P124/M124 + s * P132/M132 - P162/M162 - 1/u * P166/M166$$

$$d(Q197) = SF175 + P132/M132 + P166/M166$$

$$d(Q199) = SF173 + P110/M110 + P149/M149$$

$$d(Q195) = j * P110/M110 + P105/M105 - l * P149/M149 - P153/M153$$

$$d(Q193) = i * P110/M110 + P102/M102 - P155/M155 - k * P149/M149$$

$$d(Q183) = P57/M57 + p * P72/M72 - r * P132/M132 - P126/M126$$

$$d(Q181) = P55/M55 + o * P72/M72 - 1/q * P132/M132 - P124/M124$$

$$d(Q187) = P52/M52 + f * P63/M63 - P105/M105 - h * P110/M110$$

$$d(Q185) = P50/M50 + e * P63/M63 - P102/M102 - 1/g * P110/M110$$

$$d(Q179) = b * P2/M2 + P14/M14 - P52/M52 - d * P63/M63 - P57/M57 - n * P72/M72$$

$$d(Q177) = a * P2/M2 + P11/M11 - P50/M50 - 1/c * P63/M63 - P55/M55 - 1/m * P72/M72$$

$$d(Q92) = P2/M2 + SF88 + P72/M72$$

$$d(Q90) = P2/M2 + SF85 + P63/M63$$

$$d(Q25) = P14/M14 - SF23$$

$$d(Q26) = P11/M11 - SF28$$

$$d(Q17) = P2/M2 - SF9$$

$$d(Q207) = P52/M52 + d * P63/M63$$

Notation used in equation

P= The total integral of inertial element

Q= The integral of capacitance element

M= Mass of segment

ab,c,...w = Modulus specifier

SE = External force applied on the model

SF= External flow (velocity and angular velocity)

R= resistance element







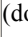







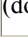











C= capacitance element




























Appendix B















B.1 Various expressions used in the modelling

Variable	Assignment
SF9 (double)	
K17 (double)	$K17=c1$;
R18 (double)	$R18=r1$;
m (double)	$m=(.1794)*(\sin(z5))$;
pelvisMOI(double)	
M2 (double)	$M2=(\text{pelvisMOI})$;
M14 (double)	$M14=M1$;
SE15 (double)	$SE15=-(M1)*(9.81)$;
SF23 (double)	
R24 (double)	$R24=r1$;
K26 (double)	$K26=c1$;
SF28 (double)	
R27 (double)	$R27=r1$;
K25 (double)	$K25=c1$;
M1 (double)	
M11 (double)	$M11=M1$;
plength(double)	
z1 (double)	
a (double)	$a=(-.042)*(\sin(z1))$;
b (double)	$b=(.042)*(\cos(z1))$;
z2 (double)	
c (double)	$c=(.18135)*(\sin(z2))$;
d (double)	$d=(-.18135)*(\cos(z2))$;
z5 (double)	
n (double)	$n=(-.1794)*(\cos(z5))$;
e (double)	$e=(-.28365)*(\sin(z2))$;

f (double)	$f = (.28365) * (\cos(z2));$
o (double)	$o = (.2806) * (\sin(z5));$
p (double)	$p = (.2806) * (\cos(z5));$
SF85 (double)	
SF88 (double)	
K90 (double)	$K90 = c1;$
R89 (double)	$R89 = r1;$
R91 (double)	$R91 = r1;$
K92 (double)	$K92 = c1;$
z3 (double)	
g (double)	$g = (.1806) * (\sin(z3));$
h (double)	$h = -(.1806) * (\cos(z3));$
i (double)	$i = -(.2494) * (\sin(z3));$
j (double)	$j = (.2494) * (\cos(z3));$
z6 (double)	
q (double)	$q = (.1806) * (\sin(z6));$
r (double)	$r = -(.1806) * (\cos(z6));$
s (double)	$s = -(.2494) * (\sin(z6));$
w (double)	$w = (.2494) * (\cos(z6));$
z4 (double)	
k (double)	$k = (.1144) * (\sin(z4));$
l (double)	$l = -(.1144) * (\cos(z4));$
z7 (double)	
u (double)	$u = (.1144) * (\sin(z7));$
v (double)	$v = -(.1144) * (\cos(z7));$
SE168 (double)	$SE168 = -(M7) * (9.81);$
LGRFINY (double)	
SE169 (double)	$SE169 = (LGRFINY);$
M170 (double)	$M170 = M7;$

 LFOOTMOI (double)	
 M166 (double)	M166=(LFOOTMOI);
 M7 (double)	
 M162 (double)	M162=M7;
 M153 (double)	M153=M4;
 RFOOTMOI (double)	
 M149 (double)	M149=(RFOOTMOI);
 M4 (double)	
 M155 (double)	M155=M4;
 M8 (double)	
 M50 (double)	M50=M8;
 M52 (double)	M52=M8;
 RTHIGHMOI (double)	
 M63 (double)	M63=(RTHIGHMOI);
 M5 (double)	
 M55 (double)	M55=M5;
 M57 (double)	M57=M5;
 LTHIGHMOI (double)	
 M72 (double)	M72=(LTHIGHMOI);
 M6 (double)	
 M124 (double)	M124=M6;
 M126 (double)	M126=M6;
 LLEGMOI (double)	
 M132 (double)	M132=(LLEGMOI);
 M3 (double)	
 M102 (double)	M102=M3;

 M105 (double)	M105=M3;
 RLEGMOI (double)	
 M110 (double)	M110=(RLEGMOI);
 RGRFINY (double)	
 SE152 (double)	SE152=(RGRFINY);
 SE151 (double)	SE151=-(M4)*(9.81);
 RGRFINX (double)	
 SE154 (double)	SE154=(RGRFINX);
 LGRFINX (double)	
 SE163 (double)	SE163=(LGRFINX);
 SE58 (double)	SE58=-(M5)*(9.81);
 SE127 (double)	SE127=-(M6)*(9.81);
 SE104 (double)	SE104=-(M3)*(9.81);
 SE53 (double)	SE53=-(M8)*(9.81);
 SF171 (double)	
 SF172 (double)	
 SF175 (double)	
 SF173 (double)	
 c1 (double)	
 K177 (double)	K177=c1;
 K179 (double)	K179=c1;
 K185 (double)	K185=c1;
 K187 (double)	K187=c1;
 K181 (double)	K181=c1;
 K183 (double)	K183=c1;
 K193 (double)	K193=c1;
 K195 (double)	K195=c1;

 K199 (double)	K199=c1;
 K197 (double)	K197=c1;
 K189 (double)	K189=c1;
 K191 (double)	K191=c1;
 r1 (double)	
 R178 (double)	R178=r1;
 R180 (double)	R180=r1;
 R182 (double)	R182=r1;
 R190 (double)	R190=r1;
 R192 (double)	R192=r1;
 R198 (double)	R198=r1;
 R200 (double)	R200=r1;
 R194 (double)	R194=r1;
 R196 (double)	R196=r1;
 R184 (double)	R184=r1;
 R188 (double)	R188=r1;
 R186 (double)	R186=r1;
 K203 (double)	K203=c1;
 K205 (double)	K205=c1;
 R206 (double)	R206=r1;
 R204 (double)	R204=r1;

References

1. P. C. Matthijsse and P. C. Breedveld “*Modelling and simulation of human gait in three dimensions using multiband graphs and implicit integration routines.*” In Congress Proceedings, 7-th Congress of the International Society of Electrophysiological Kinesiology, 1988, pages 477—480.
2. P. C. Matthijsse and P. C. Breedveld. “*Modelling and simulation of human gait in three dimensions with multiband graphs*” In Congress Proceedings, Xii International Congress of Biomechanics, Los Angeles, California, 1989, pages 208—20
3. D. A. Winter, John Wiley & Sons, “*Biomechanics and Motor Control of Human Movement*” 1990.
4. D. A. Winter “*The Biomechanics and Motor Control of Human Gait Normal, Elderly and Pathological*” University of Waterloo Press, 1991.
5. D. A. Winter “*Human balance and posture control during standing and walking*” 1995, *Gait& Posture*, **3**:193—214,
6. D. A. Winter, J. J. Eng, and M. Ishac, “*Three - dimensional movements, powers, and work in normal gait. Human Motion Analysis*” Current Applications and Future Directions, 1996, IEEE Press: 71 — 83,
7. D. C. Karnopp, D. L. Margolis, and R. C. Rosenberg, “*Systems Dynamics: A Unified Approach*” John Wiley & Sons 1990.
8. I. Kingma, M. P. de Looze, H. M. Toussaint, H. G. Klijnsma, and T. B. M. Bruijnen.”*Validation of a full body 3-d dynamic linked segment model*” 1996, *Human Movement Science*, **15**:833 — 860,
9. J. C. Pezzack and R. W. Norman. “*A validation of the joint reaction force and resultantmoment output of an ”n” link plane motion model of the human*”.
10. D. W. Risher, L. M. Schutte, and C. F. Runge. “*The use of inverse dynamics solutions in direct dynamics simulations*” 1996. *ASME Journal of Biomechanical Engineering*, **119**:417—422,
11. C L Vaughan, “*Dynamics of Human Gait (2nd edition)*” B L Davis and JCO.Connor.
12. A. D. Kuo, “*A least-square estimation approach to improving the precision of the inverse dynamics computations*” 1998 *ASME Journal of Biomechanical Engineering*, **120**:148—159,

13. C. F. Runge, F. E. Zojac, D. W. Risher, and A. E. Bryson “*Estimating net joint torques from kinesiological data using optimal linear system theory*” 1995 IEEE Transaction on Biomechanical Engineering, **42(12)**:1158—1164.
14. S.Tashman, F. E. Zojac, and I. Perakash, “*Modelling and simulation of paraplegic ambulation in a reciprocating gait orthosis*” 1995 ASME Journal of Biomechanical Engineering, **117**:300—308,
15. G. Taga. “*A model of neuro-musculo-skeletal system for the human locomotion*” 1995 IEEE Biological Cybernetics, **73**:97—111,
16. A. D. Kuo. “*A least-square estimation approach to improving the precision of the inverse dynamics computations*” 1998 ASME Journal of Biomechanical Engineering, **120**:148—159.
17. F. M. L. Amirouche, S. K. Ider, and J. Trimble. “*Analytical method for the analysis and simulation of human locomotion*” 1990 ASME Journal of Biomechanical Engineering, **112**:379—386,
18. Amalendu Mukherjee and Ranjit Karmakar – “*Bond Graph in Modeling, Simulation and Fault Identification*”
19. C. Vera. “*Simulación de sistemas dinámico mediante la técnica del BOND-GRAPH. Madrid*” ETSI Industriales, 1993.